FALCONBRIDGE

FALCONBRIDGE LIMITED

A thesis submitted in conformity with the requirements

for the Degree of Master of Applied Science

in the University of Toronto

DENSITIES OF MOLTEN COPPER-NICKEL MATTES

BY

JOHN NICHOLAS HRYN

Department of Metallurgy and Materials Science

CONTRACT SERIAL NUMBER OSQ83-00195

This work was carried out as Part B of DSS Contract 15SQ.12440-3-9172

To Develop a Clean Smelting Process for Highly Roasted Copper-Nickel Calcines

93AP

MICROMEDIA

Project: 82-600

Copies: L.E. Seeley, G.H. Kaiura, W.R. Hatch, file 82-600

ACKNOWLEDGEMENTS

The author would like to thank Prof. J. M. Toguri for helpful discussions and moral support throughout this project.

Thanks also to Dr. G. H. Kaiura, Mr. R. Hatch and other members of Falconbridge Ltd., for their technical assistance, and for providing chemical analyses.

Financial support from Falconbridge Ltd. and NSERC is appreciated.

TABLE OF CONTENTS

PAGE

Acknowledgements iii

List of Figures and Tables vi

Abstract viii

Introduction 1

Literature Survey 4

i) Capillary Rise Technique 4

ii) U-tube Technique 7

iii) Sessile Drop Technique 10

iv) Maximum Bubble Pressure Technique 12

v) Archimedean Technique 14

vi) Analyses of Techniques 17

Outline of Research Program 18

Experimental 24

i) Apparatus 24

a) Furnace 24
b) Power Considerations 27
c) Lower Drive Assembly 28
d) Upper Drive Assembly 30
e) Alumina Bobs 31
f) Gas Train 32

ii) Specimen Preparation 35

iii) Technique 40

a) Derivation of Equations 40
b) Procedure 45

TABLE OF CONTENTS (...continued) PAGE

Results 49

Discussion 58

i) Technique 58

a) Volume of Alumina Bobs 58
b) Measurements 61
c) Errors in the Measurements 64

ii) Specimen Related 66

a) Initial Compositions 66
b) Changes in Matte Composition 67
c) Sampling Methods 69

iii) Matte Density as a Function of Temperature and Composition 71

Conclusions 73

References 74

Appendicies 76

Appendix A - Initial Compositions of B-series Specimens 77

Appendix B - Target Compositions of C-series Specimens 78

Appendix C - Final Assays of Matte Specimens 79

Appendix D - Raw Data 80

LIST OF FIGURES AND TABLES

PAGE

Figure 1. Apparatus used by Bourgon et al. 5

Figure 2. Apparatus used by Travnichek and Chernomurov. 6

Figure 3. Apparatus used by Byerley and Takebe. 7

Figure 4. Sample of data obtained by Byerley and Takebe. 9

Figure 5. Apparatus used by Tokumoto et al. 10

Figure 6. Sketch of meridional section of sessile drop. 11

Figure 7. Apparatus used by Nagamori. 12

Figure 8. Apparatus used by Kaiura and Toguri. 15

Figure 9. The Cu-Ni-Fe-S composition diagram. 18

Figure 10. The (Cu+Ni)-Fe-S-O composition diagram. 19

Figure 11. Densities along the Cu_2S-Ni_3S_2 psuedo binary. 20

Figure 12. Oxygen solubility in converter mattes. 21

Figure 13. Oxygen content as a function of iron content in converter mattes. 21

Figure 14. The effect of oxygen on density. 22

Figure 15. Compositions of matte specimens investigated. 23

LIST OF FIGURES AND TABLES (...continued) PAGE

Figure 16. Apparatus. 26

Figure 17. Circuit diagram for furnace. 28

Figure 18. Bob and crucible arrangement. 33

Figure 19. Gas train. 34

Figure 20. Outline of the specimen preparation procedure. 36

Table 1. Normalized compositions and ratios of the first thirteen matte specimens. 49

Table 2. Normalized compositions and ratios of the seven synthesized matte specimens. 49

Figure 21a. Density data as a function of temperature. 51

Figure 21b. Density data as a function of temperature. 52

Table 3. Densities of the matte specimens. 53

Figure 22. Densities of the matte specimens at 1100°C. 55

Figure 23. Densities of the matte specimens at 1200°C. 56

Figure 24. Densities of the matte specimens at 1300°C. 57

Figure 25. Balance readout versus bob immersion depth. 62

ABSTRACT

A bottom-weighing Archimedean technique employing twin alumina bobs was used to determine the densities of twenty copper-nickel mattes. The specimens were held in a vertical tube Kanthal Super resistance furnace under a deoxidized argon atmosphere. The matte specimens were synthetically prepared to simulate typical industrial mattes. Copper/nickel mass ratios were held at 1:1 with the matte grade varying from 13% to 57% copper plus nickel. Oxygen was added to the mattes to correspond to an iron/oxygen mass ratio of 16:1, which is typical of industrial mattes. Densities were determined in the temperature range 1100 - 1300°C. Accuracy of the obtained density values were within 0.5%. An empirical equation relating the density of mattes to their composition and temperature was developed, and is given below:

$$\text{Density}[g/mL] = 6.532 - 0.0856 \cdot \text{mass\% S} + 0.0097 \cdot \text{mass\% (Cu + Ni)} + 0.00049 \cdot (1200 - T[C^{\circ}]).$$

RÉSUMÉ

La densité de vingt échantillons de mattes de cuivre et nickel a été déterminée par l'application du principe d'Archimède à un sytème de pesage par en bas, en opérant le déplacement au moyen d'une série de deux cylindres en alumine. Les échantillons reposaient sur un support, à l'intérieur d'un four à resistance Kanthal Super à tube vertical, dans une atmosphère désoxydée d'argon. Les échantillons de matte avaient été produits synthétiquement de façon à simuler les mattes industrielles typiques. Les proportions par masse cuivre/nickel étaient égales (1:1), tandis que la qualité de la matte variait de 13% à 57% (teneur combinée en cuivre et nickel). On a ajouté aux mattes de l'oxygène dans la proportion par masse fer/oxygène 16:1, proportion typique des mattes industrielles. Les densités ont été déterminées dans un milieu dont la température allait de 1100° à 1300° C. Les densités obtenues étaient exactes à 0,5 % près. L'équation empirique suivante, indiquant la densité des mattes par rapport à leur composition et leur température, a été établie:

$$\text{Densité [g/mL]} = 6{,}532 - 0{,}0856 \times \text{masse \% S} + 0{,}0097 \times \text{masse \% (Cu + Ni)} + 0{,}00049 \times (1200 - T[C^\circ])$$

INTRODUCTION

This thesis describes the determination of the densities of molten copper-nickel mattes. Reliable density data are presently unavailable. In cooperation with Falconbridge Ltd., the densities of several synthetic copper-nickel mattes were measured over the temperature range 1100 - 1300^{o}C. The compositions of the matte specimens were restricted to those that were considered to be most suited to the needs of the industry.

Volumes of liquids are difficult to measure due to surface and interfacial tension effects. This is the main reason that accurate density data are difficult to obtain. The determination of the densities of molten sulfides is further complicated by the high temperatures required and the necessity to control the atmosphere, since sulfur is readily oxidized to various sulfur oxides which can escape as gas and thereby change the composition of the matte specimen.

There are practical and theoretical reasons as to why density data of molten mattes are important. Density data are required in the analyses of reaction rates that occur in sulfide smelting and converting processes. For example, they can be used to establish the concentration of the melt

in terms of unit volume. This can then be used to formulate natural convective effects that arise from density changes resulting from metallurgical reactions.

Knowledge of densities could also lead to a better understanding of the phenomena which give rise to the presence of a solid magnetite phase in smelting and converting vessels. Should a solid magnetite phase form, density data can help predict its location. For example, in higher matte grades which have higher densities than that of solid magnetite, magnetite will accumulate at the matte-slag interface where it can impede the reaction rate between the matte and slag. In lower matte grades with lower densities, magnetite will accumulate at the bottom of the vessel, where it can block tuyeres and restrict the flow of oxygen. By knowing the density of the matte, detection of magnetite is facilitated.

Mass balances in pyrometallurgical plants have always been difficult to determine, yet they are important in assessing the economics of the processes. One of the major difficulties occurs in the converter aisle. The quantity of matte converted is usually recorded by the number of ladles processed. Although the volume of each ladle is known, the mass of matte in each ladle is usually estimated, since the density of the matte is unknown. Therefore, matte density data can also improve the accuracy of material balances

especially in the converter aisle.

But apart from the practical value of density data in treating matte-slag separation and transport problems, the data may provide a basis for a better understanding of the structure and bonding of molten mattes, especially when combined with data on other physical properties, such as electrical conductance, surface tension and viscosity. In that case, molar volumes, which are derived from density-composition relations, will be required. For example, metal-sulfur atomic bonding is considered to be somewhere between metallic and ionic, depending on composition and probably other variables. The radius of the S^{2-} anion was reported as 0.184 nm as compared to 0.104 nm for a singly bonded covalent sulfur atom. Without taking other atomic interactions into account, it could be argued that the partial molar volume of sulfur is larger when it is more ionic. In this way, density data, when converted to molar volumes, can help resolve the structure of these sulfide melts.

LITERATURE SURVEY

A literature survey extending back 30 years revealed that only a handful of papers have been published on the densities of molten mattes. Five methods have been used to measure matte densities: capillary rise technique, U-tube technique, sessile drop technique, maximum bubble technique, and an Archimedean technique. Each of these methods has its own advantages and disadvantages, but some are clearly superior to others. A brief summary of each technique will demonstrate this.

i) Capillary Rise Technique

In the late 1950's, Bourgon et al[1] measured the density of copper-iron sulfides over a temperature range from 1200 - 1400°C. The apparatus they used is shown in Figure 1.

The molten matte sits in an alundum crucible in an induction furnace under a helium atmosphere. A silica tube is placed into the matte. The other end of the silica tube leads to a manometer which contains silicone oil. As the furnace becomes pressurized with helium, matte is forced up the silica tube and causes a pressure change across the manometer. The height of the matte column is determined by

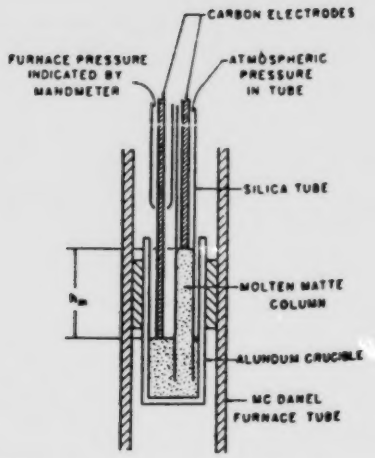

Figure 1. Apparatus used by Bourgon et al.

moving two graphite rods to the surface of the matte and testing for completion of a circuit, since molten sulfides are conductive. Because the graphite rods are of the same length, the height of the matte column can be measured from the difference in height of the ends of the graphite rods above the furnace. The density of the matte can then be determined by Equation 1, if the density and height of the silicone oil in the manometer are known.

$$D_m = D_s \times (h_s / h_m) \qquad .....1$$

where D_m is the density of the matte

D_s is the density of the silicone oil

h_m is the height of the matte column

and h_s is the height of the silicone oil

The major disadvantage with this technique is the uncertainty in the position of the matte surface. This is due to fluctuations of the surface combined with an interfacial tension effect between the graphite and sulfide. Bourgon et al estimate their error at 2%.

Travnichek and Chernomurov[2], 1973, improved this technique by using x-rays to determine the position of the matte surface, both in the crucible and in the capillary. Their apparatus is shown in Figure 2.

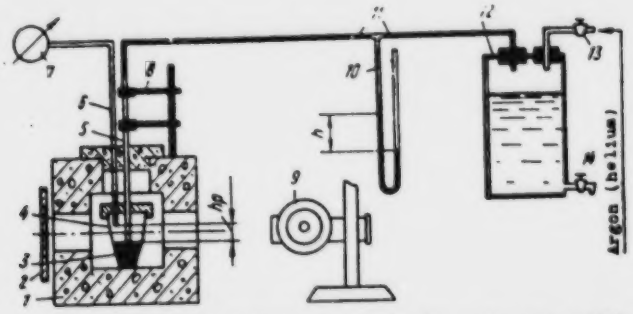

Layout of an installation used to measure melt density:
1 - high-temperature furnace; 2 - x-ray film; 3 - melt; 4 - alundum crucible with cover; 5 - quartz or alundum capillary tube; 6 - thermocouple; 7 - potentiometer; 8 - guides; 9 - type RUP-200 x-ray flaw-detector; 10- water-pressure gauge; 11 - vacuum rubber hose; 12 - container; 13, 14 - taps.

Figure 2. Apparatus used by Travnichek and Chernomurov.

Density measurements were made for Cu_2S, Ni_3S_2, and FeS at temperatures from 1200 - 1400°C. Their data are good and their error is estimated at 0.2%. Unfortunately, the exact compositions of their sulfide specimens were not reported.

ii) U-tube Technique

Byerley and Takebe[3], 1971, used a so-called U-tube method which is a variation of the capillary rise technique. Their apparatus is shown in Figure 3.

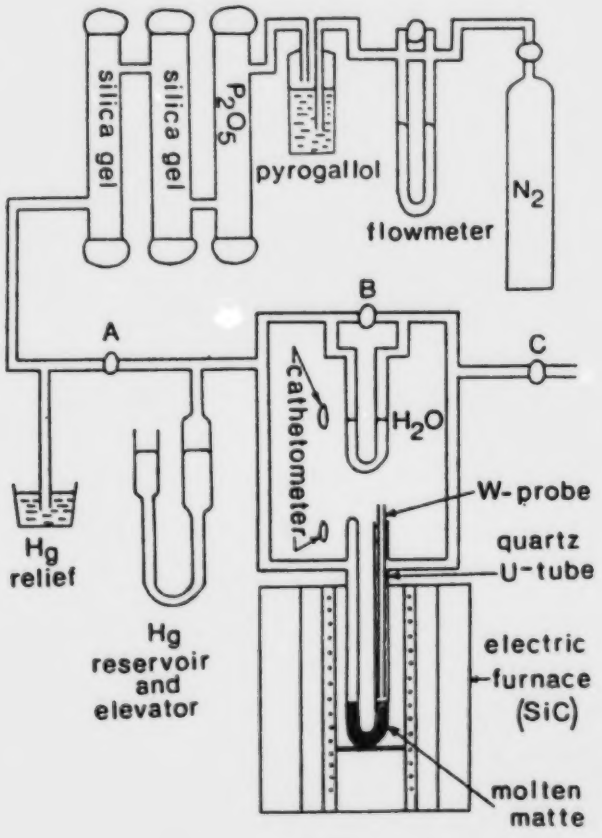

Figure 3. Apparatus used by Byerley and Takebe.

The silica U-tube was fitted with a tungsten probe which could be set at a predetermined level. After purging, stopcocks A and C were closed, which isolated a control volume. Then, after closing stopcock B, the pressure in the

left side of the apparatus was increased by raising the mercury level. When the matte rose to the preset level to complete a circuit of a lamp with the tungsten probe, the manometer level was recorded. The density could then be calculated using Equation 1, if substituting water for silicone oil.

This method apparently reduced the uncertainty of the matte column height by half because the probe is in contact with only one surface. But in order to determine the value of 'h_m' in Equation 1, the initial value of 'h' also had to be measured. It could not be calculated from the mass of the matte in the tube because the density was not known. Therefore, no real advantage is gained. This can explain why Byerley and Takebe's results are claimed to be reproducible to within 1%, but that the density values obtained are totally inconsistant with those of other authors, and do not show any logical trend. A sample of their data is shown in Figure 4.

Another problem inherent with the U-tube technique is the inability to adequately purge the atmosphere above the matte specimen. This occurs because of a pocket of stagnant gas above the matte. Any oxygen not purged from this gas will react with the sulfur in the matte and slightly change the specimen composition. But more important is the dissolution of oxygen into the matte phase

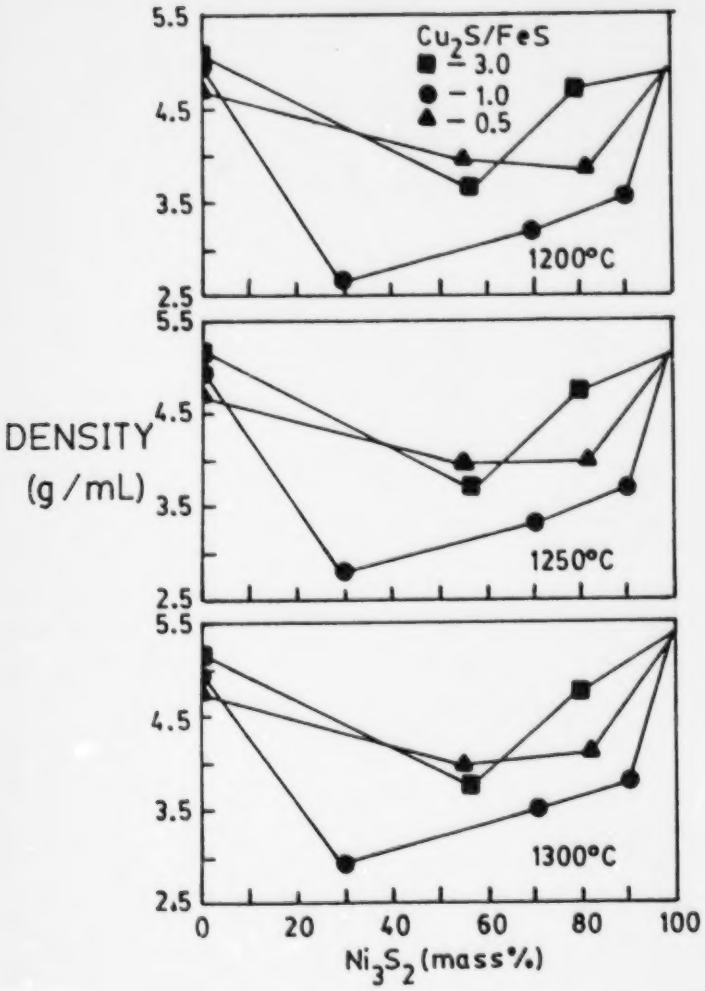

Figure 4. Sample of data obtained by Byerley and Takebe.

which increases the wettability of the silica by the matte. This will increase the error of the density value by further decreasing the apparent volume of the matte.

Azuma and Takebe[4], 1972, also used the U-tube technique to determine densities of molten copper mattes.

Their results also show scatter, but to a lesser degree than those of Byerley and Takebe. This is probably due to their improved purging technique. Nevertheless, the quality of their data seems to be inferior to those of authors who use other techniques to determine the densities of molten mattes.

iii) Sessile Drop Technique

Tokumoto et al[5], 1972, used the sessile drop method to measure the density and surface tension of copper mattes simultaneously. Their apparatus is shown in Figure 5.

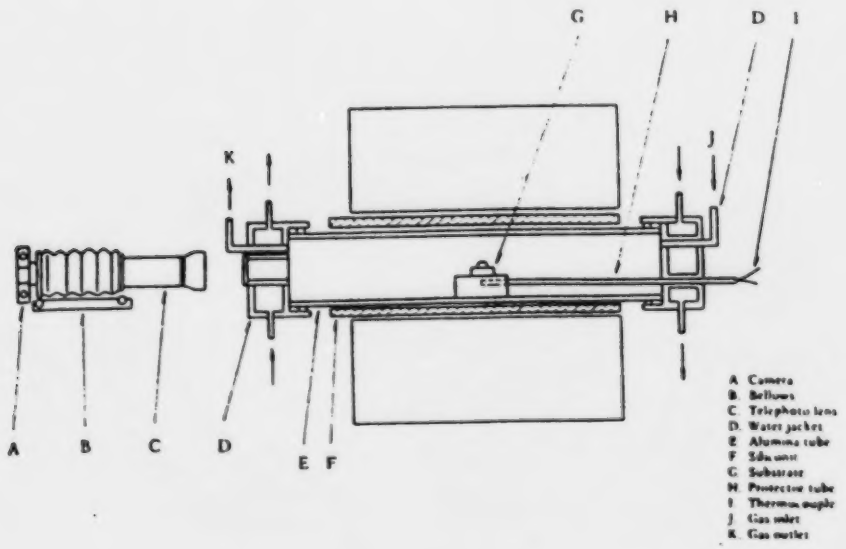

Figure 5. Apparatus used by Tokumoto et al.

The method consists of analyzing the dimensions of a sessile drop resting on a horizontal surface under an atmosphere of purified argon. The shape of the drop depends on an equilibrium between the forces of gravity and surface tension, and can be calculated from the manipulation of the Laplace equation. Bashforth and Adams[6] solved the equation and tabulated their results for values of the parameters X_1, X_2, Z_1, and Z_2, which are shown in Figure 6.

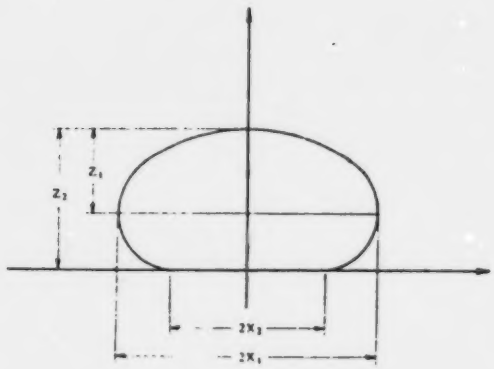

Figure 6. Sketch of meridional section of sessile drop[5].

Surface tension can be determined by measuring X_1 and Z_1, and drop volume can be determined by measuring X_2 and Z_2. Then, density could be determined from the drop mass and drop volume. But X_2 is difficult to measure precisely and the measurement is strongly dependent on human bias. The density data obtained by Tokumoto et al are about 10% lower than other authors' while the surface tension

measurements were about 10% higher. The experimental errors were estimated to be 3-4%. The discrepancies of their results were attributed to the purity of the specimens, which were reagent grade.

iv) Maximum Bubble Pressure Technique

Nagamori[7], 1969, used the maximum bubble pressure technique to measure the densities of Cu-S, Fe-S, and Ni-S systems over a wide range of temperatures and compositions. His apparatus is shown in Figure 7.

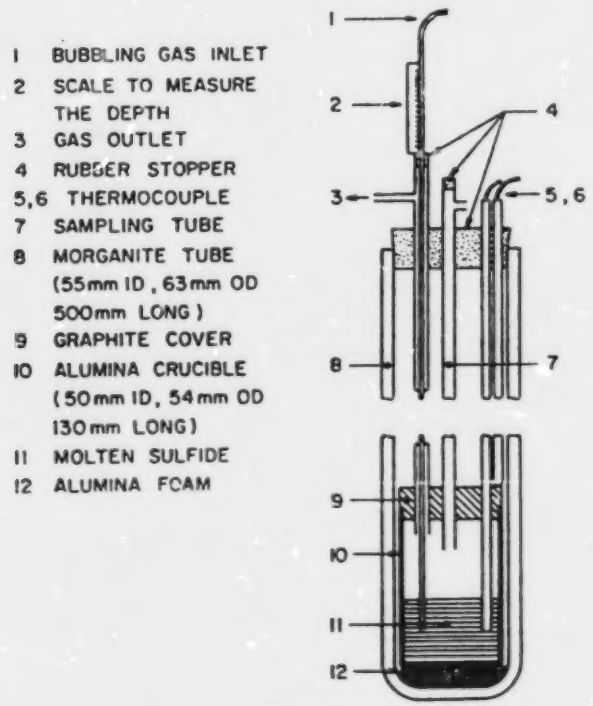

Figure 7. Apparatus used by Nagamori.

A silica tube was immersed to a known depth into the molten sulfides contained in an alumina crucible. By means of a manometer containing dibutyl phthalate, the pressure required to just force a gas bubble through the tube was measured. To minimize the variation of melt composition during a density measurement, the apparatus was constructed to allow either argon, hydrogen, hydrogen sulfide, or mixtures of these gases to be used as the bubbling gas.

In order to obtain accurate and precise data, many compensating factors have to be taken into account. These include the increase in melt level as the capillary is immersed into the melt, the volume of gas in the capillary, and the volume of the gas bubble. Another major concern is the corrosion of the silica capillary tube, since variations of the opening may cause an increase in the apparent density of the matte specimen. The results obtained by Nagamori are reasonable; the error is estimated at 0.3%.

This method seems to be preferred by many scientists in the Soviet Union. Barmin et al[8,9], 1969, 1970, and Dobrovinskii et al[10,11], 1969, 1969, measured the densities along various metal-sulfide binaries at temperatures ranging from 1200 - 1600°C. They claim their expermental error was 3-5%. However, they did not detect any variation in density with temperature. Furthermore, their precision is very low. The bubbling gas they used was

helium which has a very high heat capacity. Possibly, the helium was not up to the melt temperature and as a result localized cooling of the matte specimen near the gas bubble may have occurred. This could be one reason why a temperature dependence was not detected. The accuracy of their results must be considered suspect.

Kurochkin et al[12], 1969, measured the density of Cu_2S-FeS mixtures at 1200°C and 1300°C. The bubbling gas they used was purified argon and a temperature dependence was observed. Their experimental error is estimated at 4-6%.

Blagoveshchenskii et al[13], 1976, measured the density of some industrial mattes found in the Soviet Union. Unfortunately, the matte compositions reported were not complete, so that their work can only be considered as qualitative at best.

v) Archimedean Technique

Kaiura and Toguri[14], 1979, used a novel approach to determine the densities of molten mattes. The density of the matte was determined by measuring the buoyant force on an alumina bob of known volume. The apparatus used is shown in Figure 8.

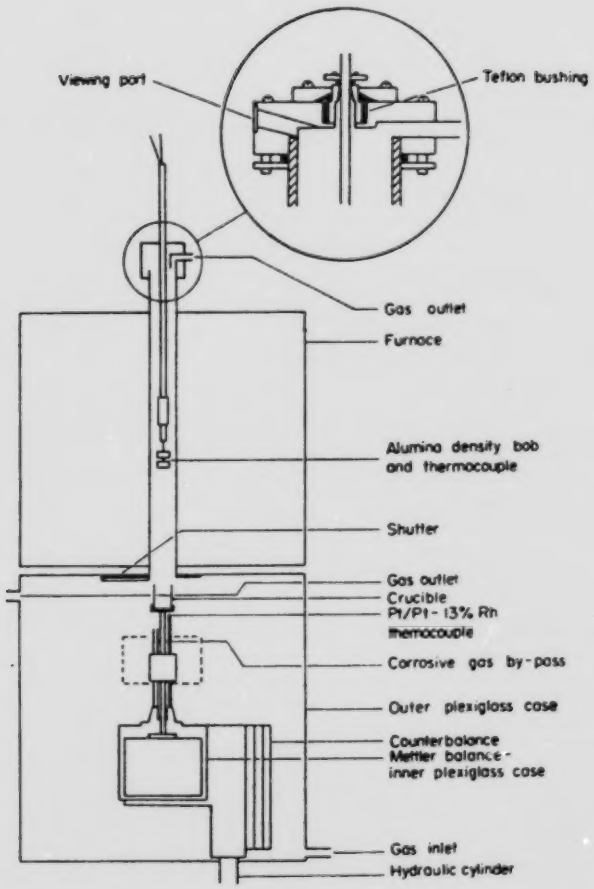

Figure 8. Apparatus used by Kaiura and Toguri.

The matte specimen was held in an alumina crucible which was supported by an alumina rod fixed to a balance, so that the weight change of the matte could be continuously measured. The entire assembly was maintained in an argon atmosphere. When the bobs in turn were immersed into the matte, the force on the balance changed.

The weight change caused by immersing the first bob is given by Equation 2, and when both bobs are immersed, the weight change is given by Equation 3. Subtracting gives Equation 4, which can be solved for the density of the matte, since the volume of the bob is known. The surface effect can also be determined by back substitution.

$$W_1/g = (V_1 \cdot D_m) + \text{surface effect} \quad \ldots\ldots 2$$

$$W_2/g = (V_2 \cdot D_m) + \text{surface effect} \quad \ldots\ldots 3$$

$$(W_2 - W_1) / g = (V_2 - V_1) \cdot D_m \quad \ldots\ldots 4$$

where $W_2 - W_1$ is the net weight change

$V_2 - V_1$ is the net volume change

and D_m is the density of the matte

The surface effect is due only to the thin alumina rod connecting the two bobs to each other and to the push-rod. Because it is the same rod with the same diameter, the surface effect associated with it can be eliminated. This method avoids the problem of the surface tension effect that occurs with some of the other techniques.

The compositions studied by Kaiura and Toguri were on the FeS-Cu_2S psuedo binary. Some density data were determined for the Fe-S-O system. The temperature range used was 1200 - 1350°C. The estimated error of their results is 2.2%.

vi) Analyses of Techniques

Only five methods have been used to date to measure the densities of molten mattes. The least accurate of these methods appears to be the U-tube technique. The capillary rise technique shows promise if the surface of the matte is recorded on x-ray film, as demonstrated by Travnichek and Chernomurov. The sessile drop method has as its main problem the sensitivity to the personal biases of the experimentor. However, the surface tension of the matte specimen can be determined simultaneously with density.

Probably the most reliable of the density data mentioned here are those obtained by Nagamori using the maximum bubble pressure technique. But it is also experimentally the most difficult, if precise and accurate data are desired. The Archimedean technique does not seem to be experimentally difficult and is the most elegant technique described here. Problems of surface tension that occur in other techniques are eliminated. It was believed that the relative experimental error reported by Kaiura and Toguri could be decreased. For these reasons it was decided to select this technique for the determination of the densities of molten mattes.

OUTLINE OF RESEARCH PROGRAM

Densities of molten mattes were measuered using a bottom-weighing Archimedean technique. The compositions of the matte specimens are in the five component system Cu-Ni-Fe-S-O. Because it is difficult to express densities in four dimensions, certain ratios were fixed to eliminate two dimensions.

The four component composition diagram Cu-Ni-Fe-S is shown in Figure 9. By setting the Cu/Ni mass ratio to 1, one dimension is eliminated. The composition diagram can then be represented by a triangle with Cu+Ni, Fe, and S on each of the three apices.

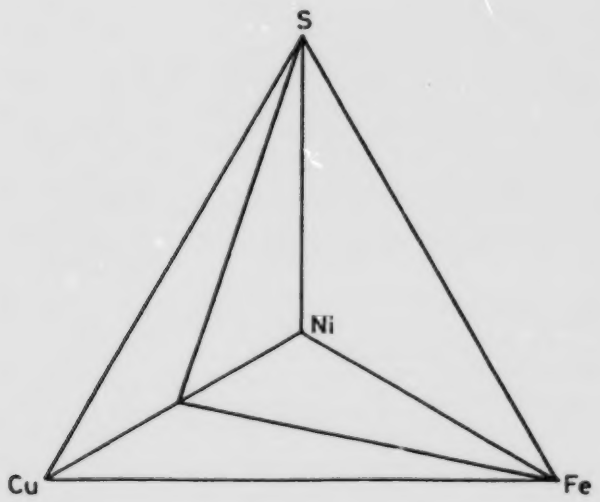

Figure 9. The Cu-Ni-Fe-S composition diagram.

Plotting this triangle against oxygen results in Figure 10. By setting the Fe/O mass ratio to 16, another dimension is eliminated. The composition of the matte specimens can now be represented on a two dimensional triangle with Cu+Ni, Fe+O, and S on each of the three apices.

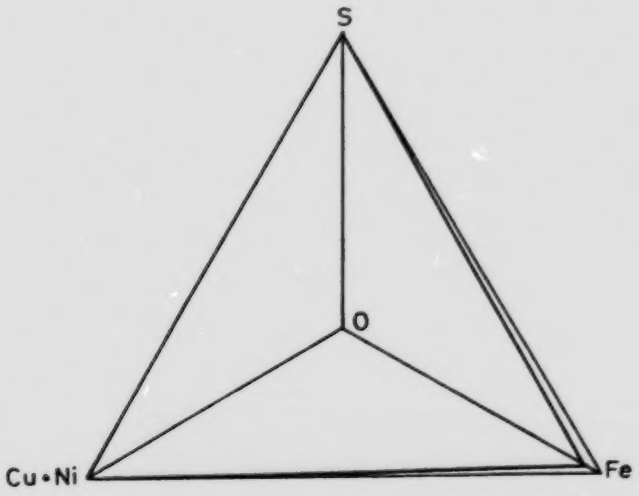

Figure 10. The (Cu+Ni)-Fe-S-O composition diagram.

The choices of the mass ratios used were primarily those of convenience. The densities along the Cu_2S-Ni_3S_2 psuedo-binary have been previously reported[9,11], and are shown in Figure 11.

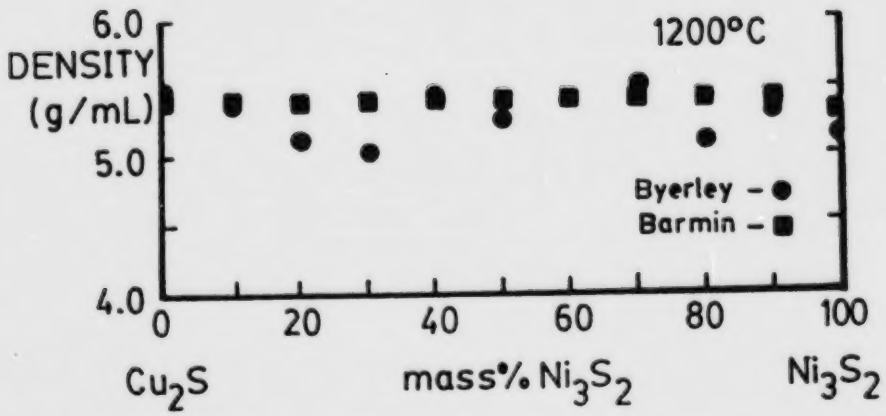

Figure 11. Densities along the Cu_2S-Ni_3S_2 psuedo-binary.

The density does not change significantly with minor deviations from the half and half mixture of the sulfides. The sulfur content of the nickel sulfide is greater than that of the copper sulfide. If the sulfur content of the nickel sulfide is lowered to that of the copper sulfide, it is believed that the density value would again not change significantly from the half and half mixture of the sulfides. It is therefore assumed that minor fluctuations in the copper/nickel ratio will not have a significant effect on the density of a matte specimen.

The Fe/O mass ratio of 16 was selected for different reasons. Figure 12 shows the typical oxygen solubility in furnace mattes[15]. The slope of the line indicates an Fe/O ratio 16 to 1. Figure 13 shows the iron and oxygen contents of the matte specimens, and their proximity to the Fe/O = 16 line.

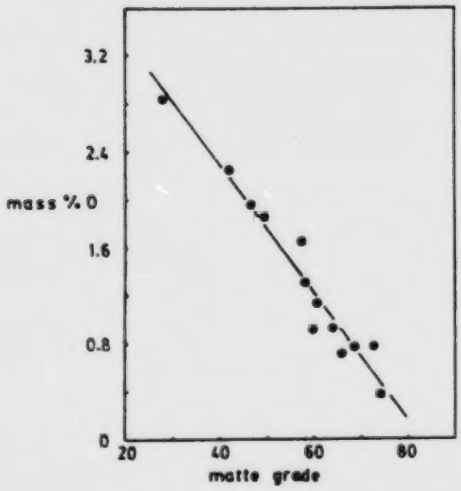

Figure 12. Oxygen solubility in converter mattes[15].

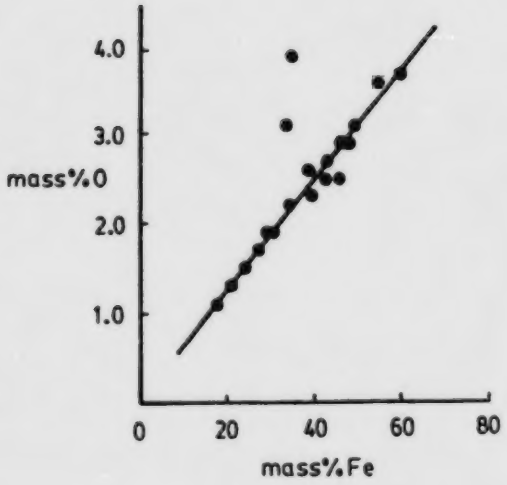

Figure 13. Oxygen content as a function of iron content in converter mattes.

Kaiura and Toguri[14] have measured the densities of iron-sulfur-oxygen mattes. Their results, seen in Figure 14, show a small dependence of oxygen on density in mattes containing low levels of oxygen. If necessary, their data can be used estimate the error in the matte specimen density values resulting from oxygen levels that are greater than those corresponding to the Fe/O mass ratio = 16. Lesser levels of oxygen appear to have little effect on the density.

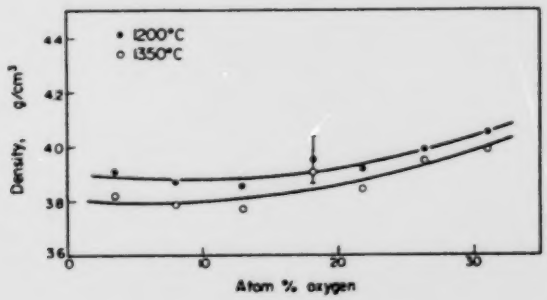

Figure 14. The effect of oxygen on density[14].

The densities of twenty matte specimens were measured in a temperature range of 1100 - 1300°C. Thirteen matte specimens along with their chemical assays were supplied by Falconbridge Ltd. The assays are tabulated in Appendix A. These specimens contained copper, nickel, iron, sulfur, and oxygen along with a few tenths of a percent cobalt. It was assumed that the cobalt content in these mattes had a negligible effect on the density because of the small relative amount. With respect to the sulfur and oxygen in

the mattes, it was assumed that cobalt behaved more like iron than either copper or nickel in these mattes. Therefore, the cobalt content was grouped with the iron content. The remaining seven matte specimens had to be synthesized from copper, nickel, iron, sulfur, and iron oxide. The compositions that were investigated are shown in Figure 15.

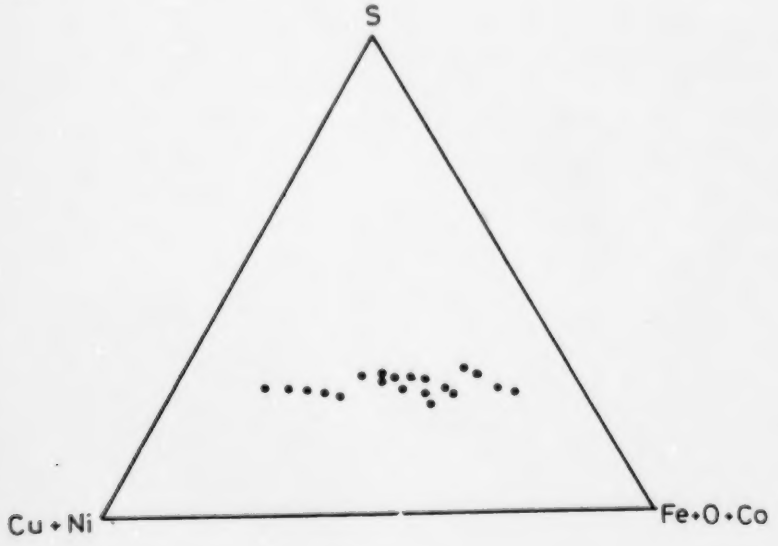

Figure 15. Compositions of matte specimens investigated.

EXPERIMENTAL

i) Apparatus

a) Furnace

An angle iron frame was constructed to hold a Kanthal Super resistance furnace in which the density measurements were to be made. Below the furnace, a drive assembly was constructed to raise the matte specimen into the furnace hot zone. Above the furnace, another drive assembly was constructed to lower the alumina bobs into the molten matte specimen in the furnace.

The furnace was constructed roughly according to a design of a vertical tube furnace as per drawings Y2-3746 in a Kanthal Super furnace design manual[16]. The dimensions of the furnace were 62 cm by 62 cm by 82 cm high, while the inner radiation cavity dimensions were 12 cm by 12 cm by 42 cm. Firebricks G30, G26, and G23, obtained from the A.P. Green Fire Brick Co., were used to brick the furnace. Transite, an asbestos board, was used as the furnace shell. The heating elements specified by the designers were not available, so minor modifications in furnace design had to be made. Four Kanthal Super heating elements were used. Their dimensions were Le=400, Lu=250, a=40, and diameters 6

and 12 mm. Each of these elements was rated at 2070 watts at 14.8 volts. The elements were placed 10 to 15 mm from the reaction tube and surrounding it. The reaction tube was made of MV30 material and was supplied by McDanel Refractories. MV30 is a fine grained mixture of 85% mullite and 15% glass. It was selected over both pure alumina and mullite compositions because of its superior thermal shock resistance. The dimensions of the reaction tube were 57 mm I.D., 63 mm O.D., and 122 cm long. The furnace is illustrated in Figure 16.

The elements were first connected to the power circuit by means of mechanically bolted copper lugs. It was not certain that these types of connections gave the necessary contact of the elements with the copper lugs in order to carry the large current required. The aluminized ends of the elements were not to exceed a temperature of 200°C because of potential damage that might occur to the aluminized contacts. Therefore, soft solder thermal breakers were installed into the power circuit near the element contacts. As the temperature of the furnace reached 1000°C, these soft solder breakers failed, indicating that localized overheating was occurring at the copper/element contact points. It was later determined that the best contact material was a tin coated braided copper wire, which had a larger contact area with the aluminized ends of the elements.

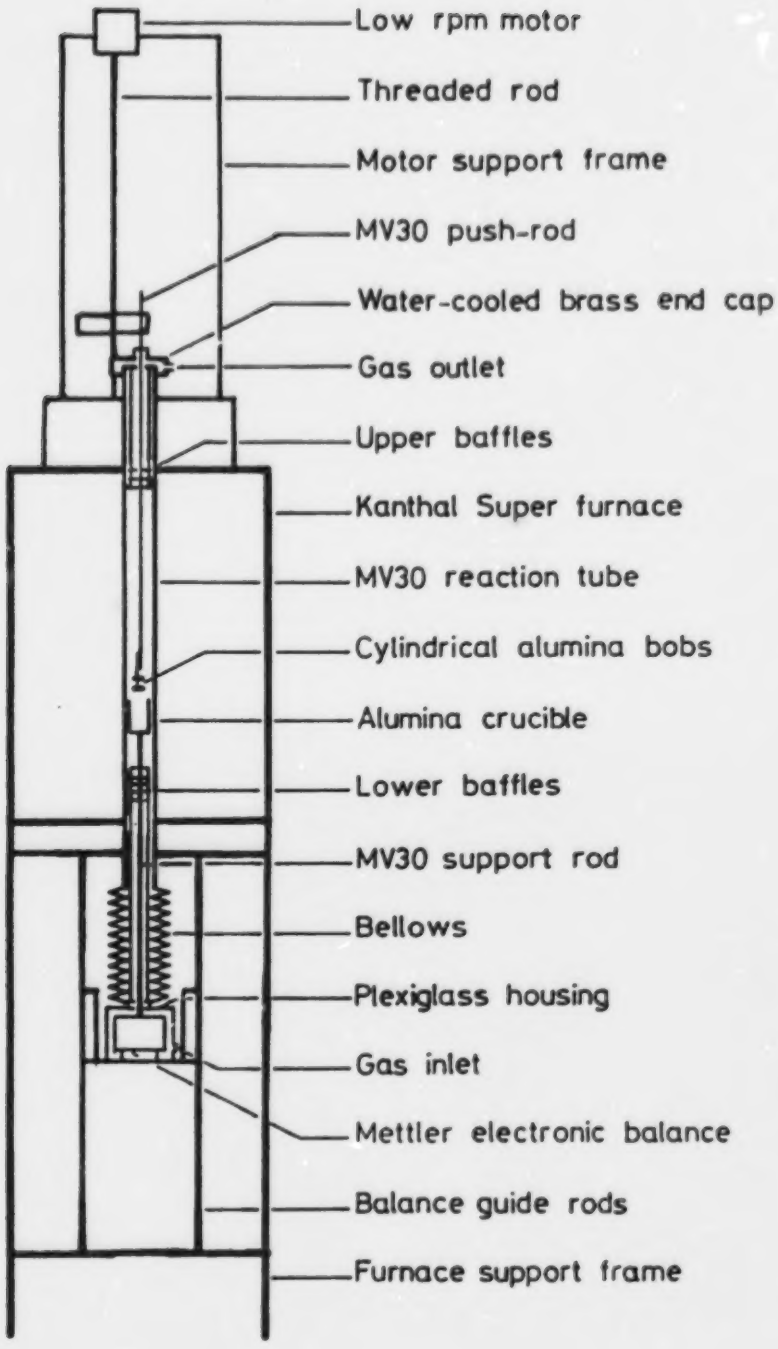

Figure 16. Apparatus.

The temperature of the furnace was indicated by a platinum / platinum-13%rhodium thermocouple placed in the inner radiation cavity of the furnace. The hot junction was in contact with the outer wall of the reaction tube in the center of the furnace hot zone. The other end of the thermocouple was connected to an Omega model 650 Type R electronic thermometer with automatic cold junction compensation.

b) Power Considerations

Power to the furnace was supplied from a 208 V, 30 A electrical outlet via two transformers. The first transformer was variable, and stepped down the voltage to 75-150 volts, depending on the power requirements of the furnace. The second transformer was fixed at a ratio of 5:2 and was used to generate the high current. The operating voltage of the four elements connected in series varied from 30 to 60 volts, depending on the furnace temperature required. The operating current remained relatively constant at 75 A at all temperatures from 1000 - 1400^{o}C. This indicated that the mode of heat loss from the furnace was primarily conduction and convection. Because the resistance of the $MoSi_2$ Kanthal Super elements increases linearly with increasing temperature, the power to the furnace varied linearly with voltage and furnace temperature. Therefore, it was not necessary to use an

automated temperature controlling device, since the temperature was easily controlled with voltage via the variable transformer. The furnace power circuit is shown in Figure 17.

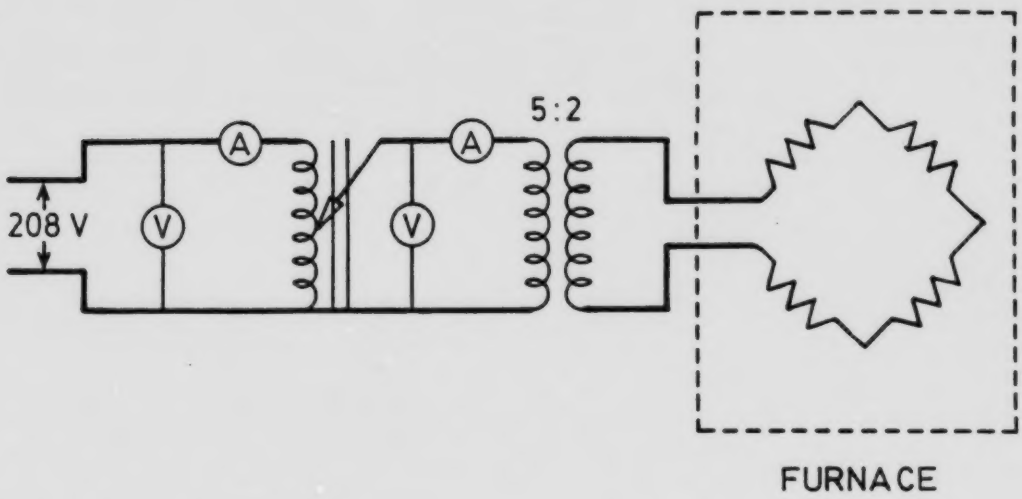

Figure 17. Circuit diagram for furnace.

c) Lower Drive Assembly

The balance used was a Mettler PL1200 top loading electronic balance. It had a readability of 0.01 grams, with a maximum capacity of 1200 grams, and a rated precision of 0.005 g. The balance was chosen because it was equipped with a vertical stability indicator which could indicate if

the crucible was in contact with the inner wall of the reaction tube while in the hot zone of the furnace. Also, a new weight reading was provided every 0.6 seconds. This response time was found to be more than adequate for that required during the measurements. An external electronic tare was also connected to the balance so that it could be zeroed remotely. The balance weighing assembly was modified to hold an 8.5 mm diameter, 56 cm high MV30 support rod with a fireclay pedestal on which a crucible containing the matte specimen was held. A splash shield was mounted on the balance in order to prevent any molten matte from coming in contact with the balance should the crucible fail in the furnace.

The balance was enclosed in a 12 mm thick plexiglass case which also served as a ballast for the incoming argon gas. The top of the plexiglass case was fitted with a water cooled brass end cap which would come in contact with the bottom of the reaction tube when the balance was raised to the 'up' position. The brass end cap also supported a series of seven Inconel 900 discs supported by three 4 mm diameter, 50 cm high Inconel rods which served as radiation baffles. A 12 mm diameter hole was drilled through the center of these baffles to allow sufficient clearance for the support rod. Also, one end of removable plastic bellows was fastened to the end cap, while the other end of the bellows could be connected to the bottom of the reaction

tube via a water cooled brass ring and a butyl rubber O-ring. This connection was made when a matte specimen was placed on the support platform with the balance in the down position, so that the atmosphere around the matte could be purged while the matte remained cool. The balance could be raised or lowered on guide rods by means of a motorized threaded rod. A counterweight was used to minimize the moment on the threaded rod.

The crucibles were made of 99.98% dense, fine grained alumina and were manufactured by Home Technics Ltd. in Peterborough. They were 78 mm high, 45 mm in diameter, and had a wall thickness of 3 mm. Alumina was selected because of its high chemical inertness. Unfortunately, alumina has rather poor thermal shock resistance properties, so that the crucible had to be raised relatively slowly into the hot zone of the furnace in order to prevent failure.

d) Upper Drive Assembly

The upper drive assembly consists of a threaded rod driven by a reversible variable speed motor. An MV30 ceramic closed end tube, 8.5 mm diameter and 92 cm long, was connected to the threaded rod by means of a cross bar. This enabled it to be moved into the furnace along guide rods in a precise and definite fashion. The top of the reaction tube was fitted with a water cooled brass end cap. The end

cap was secured to the reaction tube by means of O-ring, gas tight seals. The end cap had a centrally located opening fitted with an O-ring seal through which the ceramic push rod passed. To minimize friction restrictions, the O-ring was lubricated with a silicone based lubricant to alleviate any binding or sticking of the push rod to the O-ring.

The upper radiation baffles consisted of a series of five Inconel 900 discs with their centers cut out. They were suspended from the end cap via three Inconel rods, 4 mm in diameter and 40 cm long. The push rod, with alumina bobs attached, was eased through the centers of the radiation baffles and into the hot zone of the furnace. This was facilitated with the use of a pyrex window located on the top of the end cap.

e) Alumina Bobs

The alumina bobs were made of 99.98% fine grained dense alumina, and were also manufactured by Home Technics Ltd. The bob assembly consisted of two alumina cylinders, each 10.7 mm in diameter and 17.9 mm long, and a thin alumina rod, 1.8 mm in diameter and 100 mm long. A 2.0 mm diameter hole was electrosonically drilled through the center of one cylinder, and partially through the center of the other cylinder. The rod was passed through the hole in one cylinder and into the other cylinder. The cylinders were

adjusted with one cylinder at the bottom of the thin alumina rod, the other about 10 mm above it. This assembly was cemented in place with alumina cement and fired at 1600°C for several hours. After firing, a small amount of Aremco Ceramabond #503 alumina cement was placed on each joint between the rod and cylinders. This ensured that the molten matte would not seep into the joint during the experiments. After curing the cement, the bobs were ready to be attached to the push rod.

The bobs were fastened to the ceramic push rod via platinum and nichrome wires and cemented with Aremco Ceramabond #503 alumina cement. This ensured the bobs would not detatch from the MV30 push rod. A platinum / platinum-13%rhodium thermocouple was placed inside the push rod and was used to monitor the temperature of the melt when the bobs were immersed into the matte specimen. The bob and crucible arrangement is shown in Figure 18.

f) Gas Train

The gas used during the experiments was gettered argon. The gas train consisted of a column of drierite to remove any moisture content in the argon. A rotameter was used to control the flowrate. The gas then passed through a getter furnace filled with copper turnings. The temperature of the furnace was monitored with a chromel/alumel thermocouple and

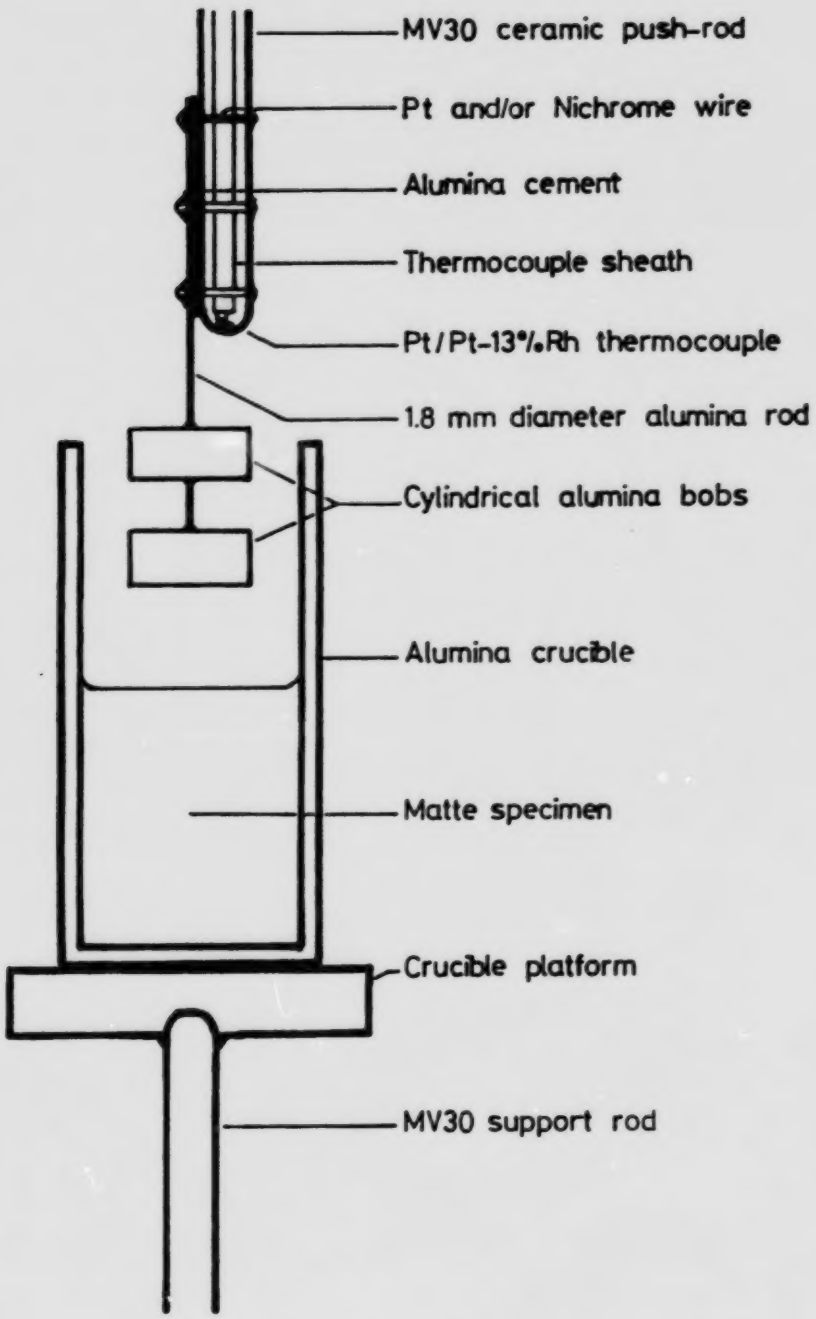

Figure 18. Bob and crucible arrangement.

controlled with a small variable transformer. A temperature of 450°C ensured that the argon atmosphere would be essentially oxygen free, that is, the residual oxygen level would be so low that it could not add significantly to the oxygen content of the samples. The gas then passed through a bubbler containing dibutyl phthalate and into the plexiglass case which housed the electronic balance. It was decided to pass the gas through the balance assembly first to prevent any corrosive sulfur gases from reaching the balance, as this could cause damage to the internal circuits of the balance. The gas then passed through the reaction tube and out through the gas exit port in the top brass end cap. Finally, the gas passed through a small bubbler filled with dibutyl phthalate and into the atmosphere of the laboratory. The bubbler prevented any oxygen from back diffusing into the reaction tube. A schematic of the gas train is shown in Figure 19.

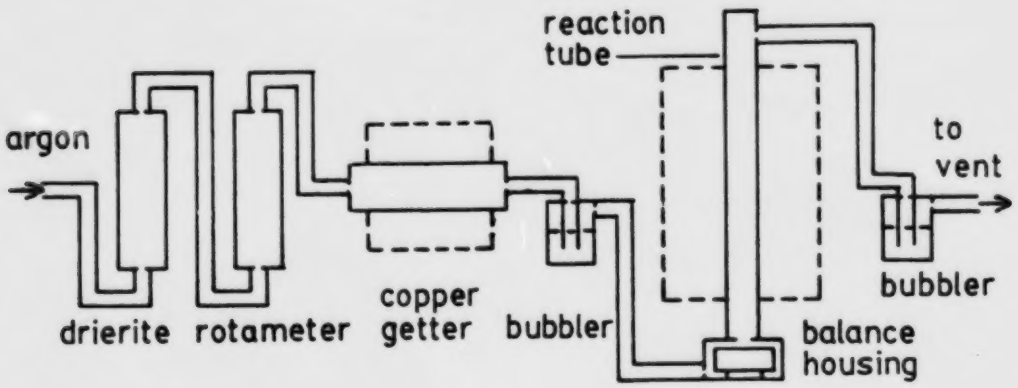

Figure 19. Gas Train.

ii) Specimen Preparation

Thirteen of the twenty matte specimens were supplied by Falconbridge Ltd. These specimens were made by adding small amounts of copper, nickel, and sulfur to several electric furnace mattes and fusing the mixtures at 1500°C in an induction furnace under an air atmosphere. This method produced low grade matte specimens with oxygen contents typical of those found in furnace mattes. Because the starting material was an electric furnace matte, the specimens also contained a few tenths of a percent cobalt. About 220 grams of each matte specimen were provided along with the chemical assays, which are tabulated in Appendix A.

The remaining seven matte specimens were synthetically produced in the laboratory. The starting materials for these mattes were commercially pure electrical grade copper, electrolytic nickel, electrolytic Armco iron, technical grade magnetite, and sublimed flowers of sulfur. The nickel and iron were supplied by Falconbridge Ltd. The sulfur was obtained from BDH Chemicals. The matte specimens were made individually by combining synthetically prepared copper, nickel, and iron sulfides, with magnetite. The target compositions, as well as the amounts of starting materials required for each of the matte specimens are tabulated in Appendix B. An outline of the procedure for preparing each matte specimen is shown in Figure 20.

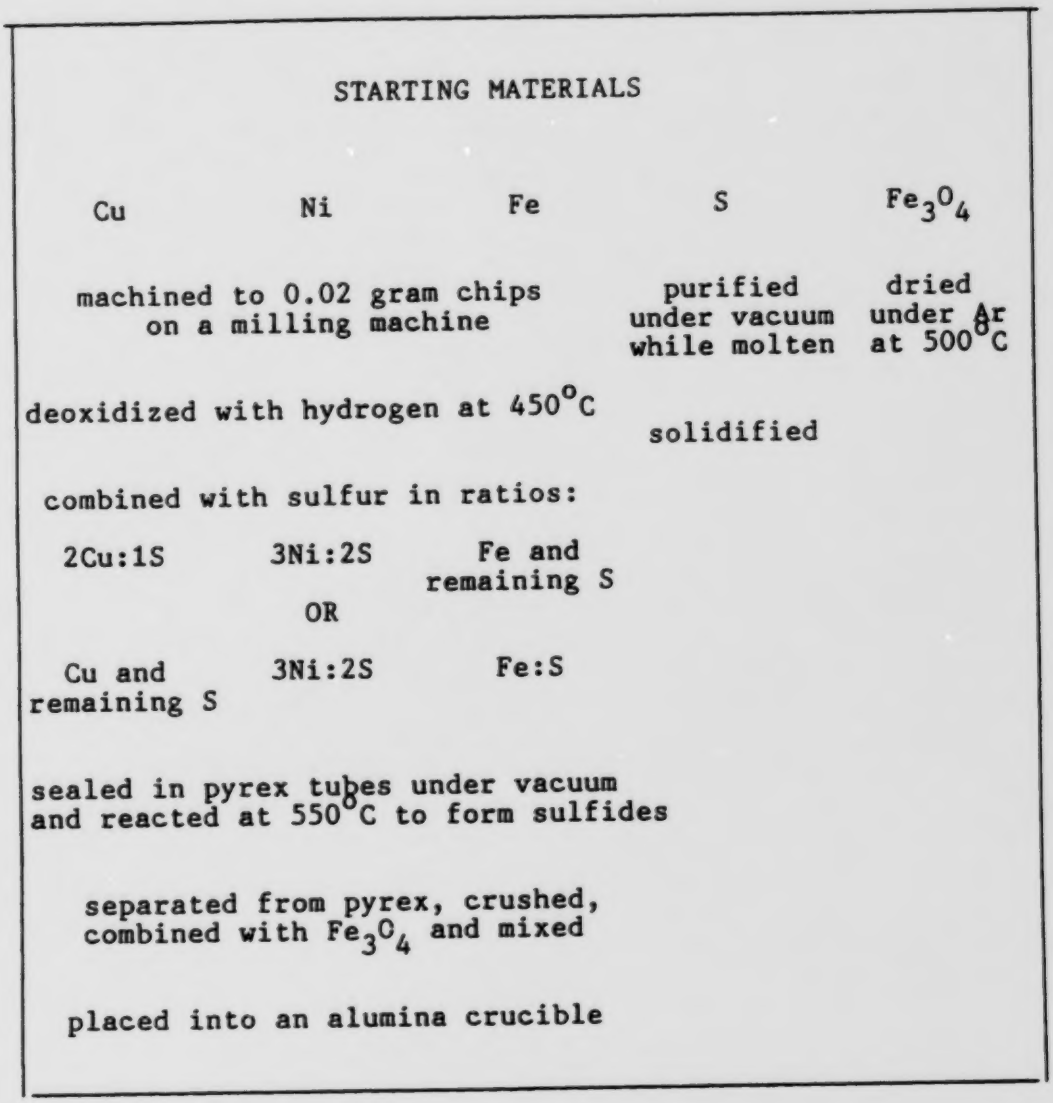

Figure 20. Outline of the specimen preparation procedure.

The first step in the procedure was to prepare the starting materials. The purity of the metals was sufficient for the determination of matte densities. Copper, nickel, and iron were machined into 0.02 gram chips on a milling

machine. The size of the metal chips turned out to be an important parameter, as will be discussed later. After milling, the copper, nickel, and iron chips were deoxidized with hydrogen at 450°C because during milling in air, the metal chips may have reached a high enough temperature to partially oxidize. This was especially true for the iron chips. After deoxidation, the metal chips were combined with sulfur.

The sulfur that was used had a purity of about 98%, with most of the impurities being carbonaceous matter. The sulfur was purified by melting it in a pyrex tube under vacuum to remove the volatile organic materials and adsorbed water. The sulfur was kept molten and under vacuum until it appeared transparent. Solidification was allowed to occur in the pyrex tube. The tube was then broken and separated from the sulfur. This resulted in large pieces of relatively pure sulfur that were much easier to handle than the fine sulfur flowers. The procedure left the sulfur ready to be combined with the metal chips.

The purity of the magnetite was unknown, but was believed to be 85-95%. Magnetite was used to set the oxygen level in the matte specimens, so only small amounts of magnetite were required. It was believed that the magnetite could be made sufficiently pure for this purpose. The main impurity in the magnetite was adsorbed water. Therefore,

purifying was done by heating the magnetite to 500°C under an argon atmosphere. A rough mass balance calculation indicated that the water content in the initial magnetite was about 5%.

The next step was to produce the metal sulfides. Copper for one matte specimen was placed into a pyrex tube with enough sulfur to produce stoichiometric Cu_2S. A required amount of nickel and sulfur to produce stoichiometric Ni_3S_2 was placed into a second pyrex tube. Some of the required iron needed to make a matte specimen would be added as magnetite. The remaining required iron was placed into a third pyrex tube with the remaining required sulfur only if the overall composition in the tube did not contain more sulfur than was needed to form stoichiometric FeS. Otherwise, only the amount of sulfur needed to make stoichiometric FeS was used. The remaining required sulfur was added to the tube containing copper and sulfur. The sulfur was distributed in this way because of the kinetics involved in synthesizing the different metal sulfides. The reaction rate of copper and sulfur is greater than that of nickel and sulfur, and much greater than that of iron and sulfur. These differences result primarily from differences in the sulfide crystal structures.

The three pyrex tubes containing the metal-sulfur mixtures were sealed under vacuum. Each tube was then

placed into a small furnace at 550°C in such a way as to have one end of the tube outside the furnace at room temperature. Sulfur exerts a pressure of one atmosphere at 445°C. But because it is allowed to condense at the cold end of the tube, the pressure can be kept relatively low by controlling the amount of gaseous sulfur at the hot end of the tube. By keeping one end of the tube at a high temperature (550°C), the poor kinetics of the reaction at low temperatures can be overcome. But by keeping the other end of the tube at room temperature, the amount of sulfur at the reaction site, and hence, the reaction rate, can be easily controlled.

The metal-sulfur reaction is extremely exothermic and autogeneous once started. If the metal chips are too small, the temperature at the reaction site can increase rapidly because of the high surface to volume ratio of the chips. If the metal chips are too large, the reaction rate decreases, as diffusion must occur through a relatively thick sulfide outer shell. It was found that sulfides could be made within a few hours at 550°C in a controlled manner if the size of the metal chips was small and had masses in the order of 0.02 grams. The whole procedure of making sulfides is a compromise between control of the reaction and the reaction rate. Acceptable control of the reaction was achieved at 550°C, and, at this temperature, the reaction rate was fairly rapid.

After all of the sulfur had reacted with the metal, the tube was cooled slowly to prevent the pyrex from cracking due to thermal shock. Also, this prevented the matte from adhering to the inner wall of the tube. The relatively greater thermal contraction of the sulfides compared to the pyrex combined with the adhesion of the sulfides to the glass can cause failure due to cracking during cooling.

After the sulfides had cooled, they were separated from the pyrex tube and weighed to determine the amount of material lost. In all cases, over 99.9% of the material was recovered. The three sulfides that pertained to one matte specimen were combined, crushed, mixed with the appropriate amount of magnetite, and placed into a crucible. The volume of the crucible was sufficient to hold the 250 g of the sulfide and magnetite mixture. Final matte synthesis would occur at the same time the densities of the matte specimens were to be measured.

iii) Technique

a) Derivation of Equations

Archimedes' principle states that the density of an object can be determined by measuring the net gravitational force on the object while it is immersed in a fluid of known density. This value is then compared to one obtained with

the object in a vacuum. Archimedes discovered this principle by weighing a gold crown in water, and then in air. He determined that the crown was actually made of a gold alloy, with a density less than that of pure gold. (The metallurgist who made the crown has not been heard from since.)

The net gravitational force on an object immersed in a fluid, or the weight of the object, is determined from its mass subtracting the mass of the fluid the object displaces, and multiplying by 'g', the acceleration due to gravity. If the fluid is air, the displaced mass is usually small and is often ignored. The density of the object is then determined using Equation 6.

$$M = W_f/g + V \cdot D_f$$

And:

$$M = W_a/g + V \cdot D_a$$

where: M = mass of an object

V = volume of the object

W_a = weight of the object in air

W_f = weight of the object in a fluid

D_a = density of air

D_f = density of the fluid

Therefore:

$$W_f/g + V \cdot D_f = W_a/g + V \cdot D_a$$

$$V = (W_a/g - W_f/g) / (D_f - D_a) \qquad \text{.....5}$$

Also:

$$V = (M - W_f/g) / D_f = (M - W_a/g) / D_a$$

$$(M - W_f/g) / D_f = (M - W_a/g) / D_a$$

$$M \cdot (D_a - D_f) = (D_a \cdot W_f/g) - (D_f \cdot W_a/g)$$

$$M = [(D_a \cdot W_f/g) - (D_f \cdot W_a/g)] / (D_a - D_f)$$

$$D = M / V$$

$$D = [(D_a \cdot W_f/g) - (D_f \cdot W_a/g)] / (W_f/g - W_a/g) \qquad \text{.....6}$$

If the volume of an object is known, the density of a fluid can be determined by using Equation 5 above, if the object is denser than the fluid. Otherwise, the object will float like a bob. In that case, the fluid must be weighed in a crucible, for example, with the bob forcibly immersed into the fluid. The density of the fluid can then be determined using Equations 7a and 7b.

mass of crucible (in air) including sample $= W_c/g + (V_c \cdot D_a)$

mass of crucible with bob immersed $= W_{cb}/g + W_b/g + [(V_c + V_b) \cdot D_a]$

mass of bob (immersed in fluid) $= W_b/g + (V_b \cdot D_f)$

where: W_c = weight of crucible and sample (in air)

W_{cb} = weight of crucible and sample with bob immersed

W_b = weight of bob immersed in fluid

V_c = volume of crucible and sample

V_b = volume of bob

Therefore:

$$W_c/g + V_c \cdot D_a + W_b/g + V_b \cdot D_f = W_{cb}/g + W_b/g + (V_c+V_b) \cdot D_a$$

$$V_c \cdot D_a + V_b \cdot D_f - (V_c+V_b) \cdot D_a = W_b/g - W_b/g + W_{cb}/g - W_c/g$$

$$V_b \cdot (D_f - D_a) = W_{cb}/g - W_c/g \qquad .....7a$$

$$D_f = [(W_{cb}/g - W_c/g) / V_b] + D_a \qquad .....7b$$

Equations 7a and 7b were utilized in the calculation of the densities of the matte specimens.

The measured value 'W_{cb}' in Equation 7b includes a term associated with a surface tension effect, which leads to an erroneous value of the fluid density. The bob is connected to a thin rod which penetrates the fluid surface. If the interfacial tension between the rod and fluid is identical to the surface tension, the magnitude of the surface effect would be zero. Otherwise, this surface effect would have a positive or negative value, depending on the wetting characteristics of the rod with the fluid. However, this effect can be eliminated by measuring two values of 'W_{cb}' with two bobs connected by a vertical rod of the same

material and diameter as the rod supporting the upper bob, as shown in Figure 18. By subtracting two equations, one applying when only the lower bob is immersed and the other when both bobs are immersed, a net 'W_{cb}' value can be obtained from the volume of the upper bob with a net zero surface effect contribution. The density of the fluid can then be obtained free from surface effect contributions. This is illustrated in the derivation of Equations 8a and 8b from Equation 7a.

With only one bob immersed:

$$W_{cb}(1)/g - W_c/g = [V_b(1) \cdot (D_f - D_a)] + \text{surface effect at rod connecting the two bobs}$$

With both bobs immersed:

$$W_{cb}(2)/g - W_c/g = [V_b(2) \cdot (D_f - D_a)] + \text{surface effect at rod supporting the upper bob}$$

where: $W_{cb}(1)$ = weight of crucible with lower bob immersed

$W_{cb}(2)$ = weight of crucible with upper bob immersed

$V_b(1)$ = volume of lower bob

$V_b(2)$ = volume of both bobs

Subtracting:

$$W_{cb}(2)/g - W_{cb}(1)/g = [V_b(2) - V_b(1)] \cdot (D_f - D_a) \quad ..8a$$

$$D_f = [(W_{cb}(2)/g - W_{cb}(1)/g) / (V_b(2) - V_b(1))] + D_a \quad ..8b$$

As evident in Equation 8b, only the volume of the upper bob, i.e., $[V_b(2) - V_b(1)]$, had to be determined in order to calculate the density of the matte specimen. The volume of the bob was determined using mercury as the fluid in Equation 8b. Mercury was selected because its density is high and well established in the literature[17]. Because of its high density, the magnitude of '$W_{cb} - W_c$' is large, which increases the precision in calculating the volume of the second bob. Also, the density of air becomes insignificant when compared to the density of mercury, so the value of 'D_a' in Equation 8b can be set to zero.

From Equation 8a above:

$$W_{cb}(2)/g - W_{cb}(1)/g = [V_b(2) - V_b(1)] \cdot [D_f - D_a]$$

Let:

D_f = density of mercury
= D_{mer}

D_a = density of air
= 0

$W_{cb}(2) = W_4$
= weight of crucible with both bobs immersed

$W_{cb}(1) = W_3$
= weight of crucible with lower bob immersed

$V_b(2) - V_b(1)$ = volume of upper bob
= V_{bu}

Therefore:

$$W_4/g - W_3/g = V_{bu} \cdot D_{mer}$$

$$V_{bu} = (W_4 - W_3)/g \; / \; D_{mer} \qquad \text{.....9}$$

After determining the volume of the upper bob at room temperature, the volume of the bob at high temperatures must be calculated. The bobs were made of high purity dense alumina with a thermal expansion coefficient of 8.5×10^{-6} per degree, as stated by the manufacturer. The bobs can be approximated to spheres in shape, so that the volume of the bobs at high temperatures can be calculated by Equation 10.

Let the volume of the upper bob at room temperature = V_o

$$V_{bu} = V_o \cdot [1 + ((8.5 \times 10^{-6}) \cdot (t - rt))]^3 \quad .....10$$

where:

t = bob temperature in degrees C
rt = room temperature in degrees C

b) Procedure

With the volume of the second bob calculated, the densities of the matte specimens can now be determined. The bobs, attached to the upper MV30 push rod, are placed into the furnace through the top end cap. The push rod is connected to the upper drive assembly so as to lower the bobs into the furnace in a slow and precise manner. With the bobs lowered, the opening through which the push rod passes is sealed by means of an O-ring. The rod is lubricated with a silicone based lubricant to prevent it from sticking to the O-ring while maintaining a gas tight seal.

the inner wall of the reaction tube, and the bobs could be immersed into the matte specimen without coming into contact with the inner wall of the crucible. This also allows the alumina bobs to equilibrate thermally with the surroundings. The bobs are then totally immersed into the matte specimen and withdrawn. This mixing action ensures that the matte is homogeneous. This also wets the bobs with the matte and deposits a thin film of molten matte onto the surface of the bobs. Also, a small drop of matte is left hanging from the bottom of the first bob. This procedure left the bobs and matte specimen ready for obtaining the data required for the density calculations.

With the balance zeroed, the bobs were immersed into the matte in 1.4 mm increments. After each increment, the weight change indicated by the balance was recorded. When both bobs were fully immersed, the temperature indicated by the thermocouple in the push rod was recorded. The position of the thermocouple at that time was a few millimeters above the surface of the matte. Therefore, the temperature recorded was assumed to be that of the specimen. The bobs were then withdrawn from the matte and the overall weight change recorded. This weight change was assumed to be the result of sulfur evolution from the matte specimen. Usually, this weight change was zero. However, when the weight change was large (in the order of 0.05 g), the data were adjusted assuming uniform sulfur evolution during the

measurements. The procedure was repeated two or three times at the same temperature.

The measurements were first made at a temperature of about 1300°C. The temperature was then lowered some 50 degrees and after thermal equilibration, the above procedure was repeated. When the bobs were immersed into the matte and then withdrawn, the size of the matte droplet on the bottom of the first bob had increased because of the change in surface tension of the matte at the lower temperature. The extent of sulfur evolution at the lower temperatures was considerably less than at higher temperatures. Overall weight losses never exceeded 0.02 g.

With the completion of the measurements at about 1250°C, the furnace temperature was lowered in about 50 degree decrements with measurements taken at each temperature level. The final measurements were taken at about 1100°C. The matte specimen was then slowly lowered out of the furnace and replaced with another matte specimen. The entire procedure was then repeated for all matte specimens. Representative matte samples were then obtained from each specimen for chemical analyses.

RESULTS

The results of the chemical analyses of the twenty matte specimens, as received from Falconbridge Ltd., are tabulated in Appendix C. The assays were normalized and grouped, as previously mentioned, and are listed in Tables 1 and 2. The ratios of the grouped elements are also shown.

Table 1. Normalized compositions and ratios of the first thirteen matte specimens.

SPECIMEN NUMBER	COMPOSITIONS (mass %)			RATIOS	
	Cu+Ni	Fe+O(+Co)	S	Cu/Ni	Fe(+Co)/O
B3	35.9	35.8	28.3	1.02	18.9
B6	16.6	53.3	30.1	0.99	14.1
B7	20.3	51.9	27.8	0.98	14.4
B12	24.5	49.3	26.2	0.97	20.3
B13	26.6	45.7	27.7	0.98	18.2
B14	29.5	42.4	28.1	0.97	17.6
B16	33.1	38.2	28.7	0.99	17.8
B17	33.0	41.6	25.4	0.96	21.1
B18	35.2	37.3	27.5	0.97	19.1
B19	38.3	33.1	28.6	0.98	20.3
B20	15.7	58.8	25.5	0.94	16.6
B21	23.7	52.1	24.2	0.94	23.4
B22	28.1	46.4	25.5	0.99	21.1

Table 2. Normalized compositions and ratios of the seven synthesized matte specimens.

SPECIMEN NUMBER	COMPOSITIONS (mass %)			RATIOS	
	Cu+Ni	Fe+O	S	Cu/Ni	Fe/O
C16	44.4	30.0	25.6	0.97	23.8
C17	46.8	27.3	25.9	1.01	18.7
C18	50.0	23.7	26.3	1.01	23.3
C19	53.3	20.0	26.7	0.98	32.7
C20	57.0	16.3	26.8	0.88	36.6
C24	29.6	46.8	23.6	1.01	25.9
C25	13.3	60.9	25.8	0.99	27.0

The densities of the matte specimens were evaluated using Equation 11.

$$D_{matte} = [(W_2-W_1)/g] \;/\; V_{bu}$$
$$= [(W_2-W_1)/g] \;/\; [V_o \cdot [1+(LCTE_a \cdot (t-25))]^3]$$
$$= \frac{(W_2 - W_1)}{(W_4 - W_3)} \cdot \frac{D_{mer}}{[1+(LCTE_a \cdot (t-25))]^3} \quad \ldots\ldots 11$$

where:

D_{matte} = the density of the matte specimen

W_2 = the net weight change recorded with both bobs immersed into the matte

W_1 = the net weight change recorded with the lower bob immersed into the matte

W_4-W_3 = the net weight change recorded with the upper bob immersed in mercury during calibration of bob volume

D_{mer} = the density of mercury = 13.546 g/mL

$LCTE_a$ = the linear coefficient of thermal expansion of the alumina bobs

$= 8.5 \times 10^{-6} / C^o$

t = the temperature of the matte specimen in C^o at the time the measurements were taken

The values of '$(W_4-W_3)/g$', 't', 'W_1/g', 'W_2/g', '$(W_2-W_1)/g$', and 'D_{matte}' for each measurement are listed in Appendix D. Figures 21a and 21b show the density data of the matte specimens as a function of temperature.

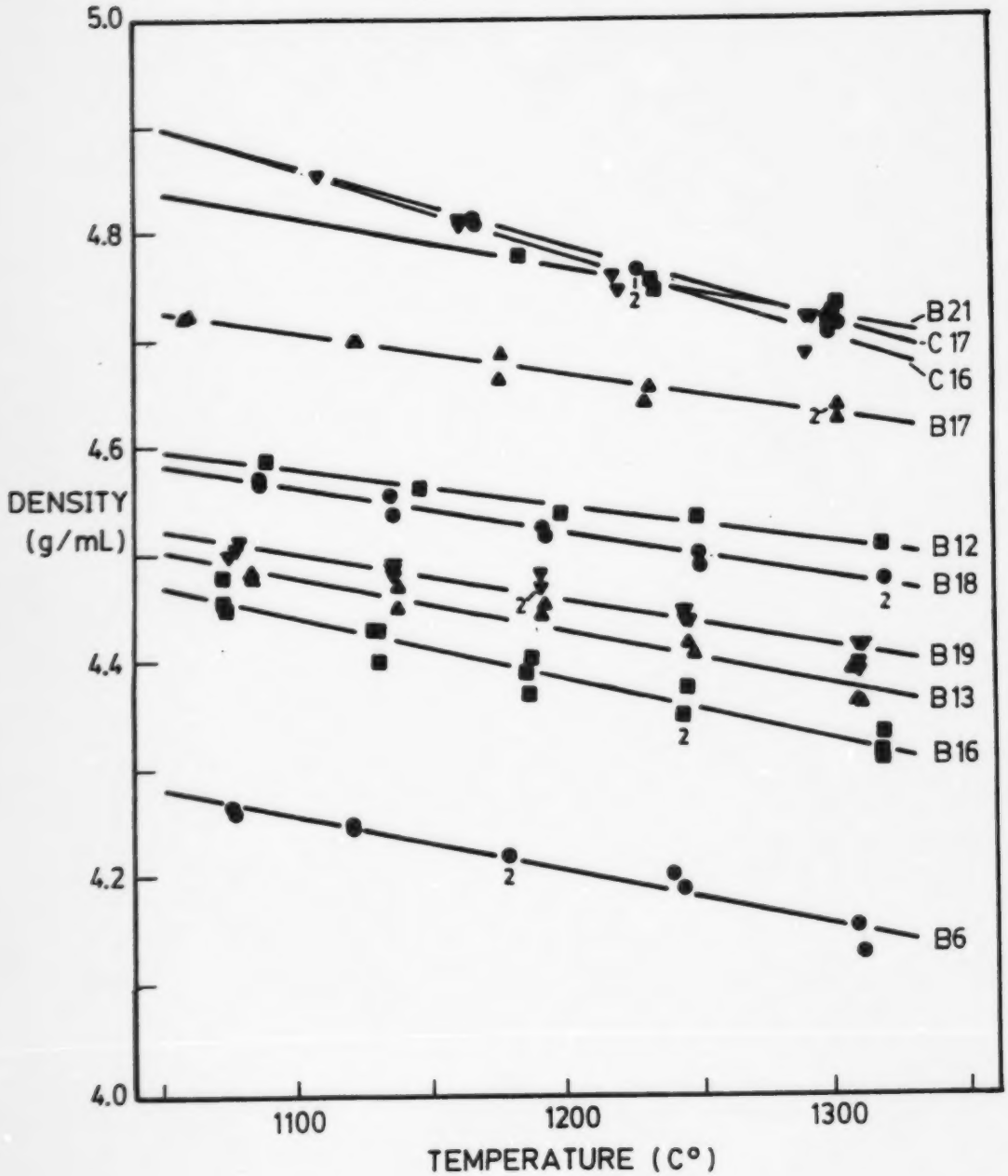

Figure 21a. Density data as a function of temperature.

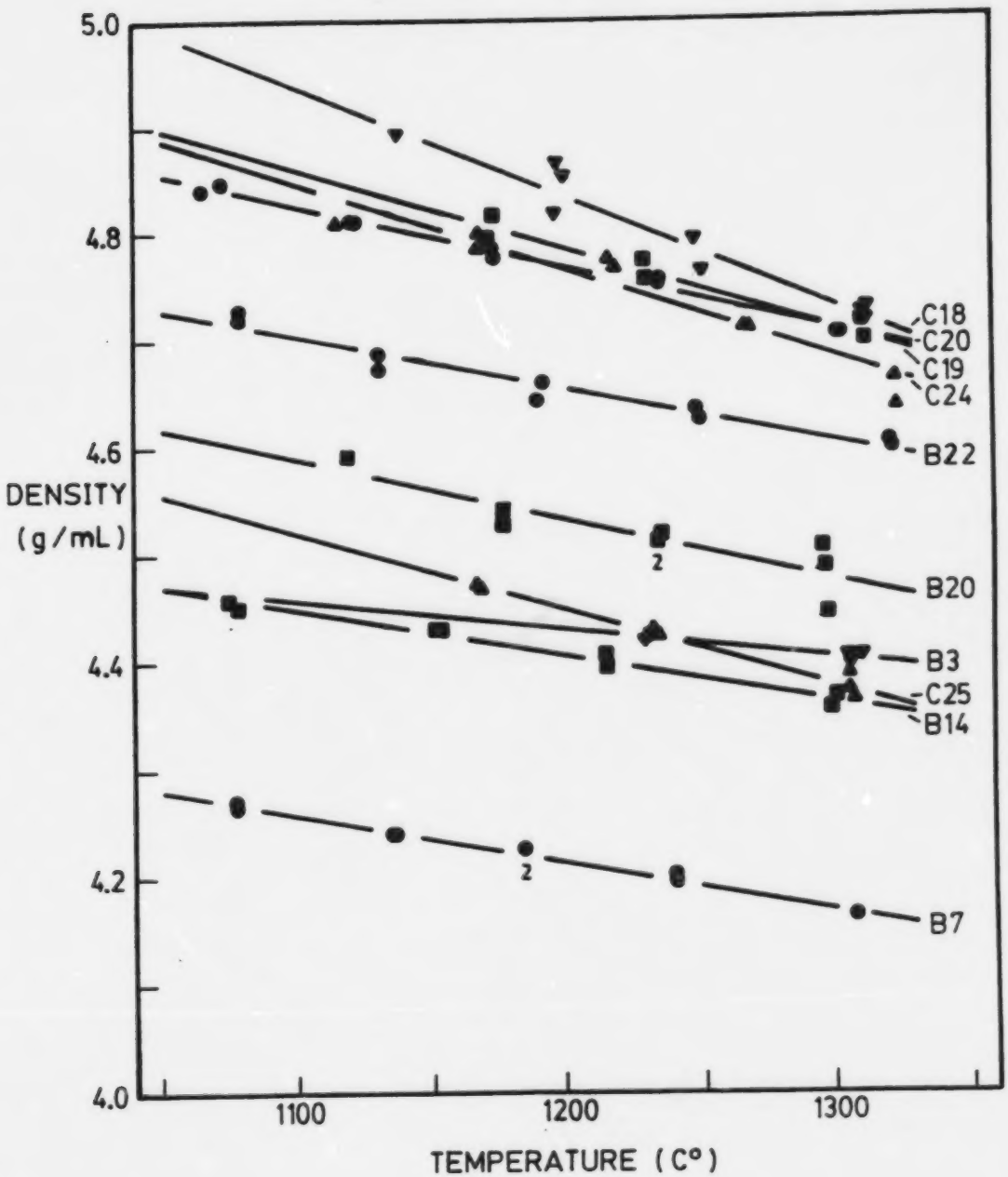

Figure 21b. Density data as a function of temperature.

The densities of the matte specimens at 1100°C, 1200°C, and 1300°C were calculated by linear regression of the raw data in Appendix D. The densities, standard errors of estimate, the correlation coefficient 'R', and the temperature coefficient 'Alpha' of each matte specimen are listed below in Table 3.

Table 3. Densities of the matte specimens.

SPECIMEN NUMBER	DENSITY			STD ERROR OF ESTIMATE	R	ALPHA x1000
	1100°C	1200°C	1300°C			
B3	4.459	4.432	4.404	0.004	0.954	0.275
B6	4.258	4.207	4.155	0.010	0.979	0.512
B7	4.260	4.216	4.172	0.003	0.996	0.444
B12	4.580	4.546	4.512	0.005	0.988	0.340
B13	4.477	4.428	4.379	0.011	0.943	0.491
B14	4.450	4.407	4.364	0.007	0.987	0.426
B16	4.441	4.384	4.327	0.014	0.968	0.574
B17	4.706	4.668	4.629	0.008	0.977	0.385
B18	4.562	4.521	4.479	0.007	0.984	0.418
B19	4.503	4.459	4.414	0.010	0.970	0.444
B20	4.587	4.532	4.477	0.018	0.888	0.547
B21	4.814	4.768	4.723	0.008	0.948	0.454
B22	4.705	4.656	4.607	0.011	0.975	0.490
C16	4.861	4.787	4.714	0.005	0.995	0.737
C17	4.858	4.779	4.700	0.014	0.974	0.789
C18	4.941	4.838	4.736	0.016	0.973	1.028
C19	4.860	4.788	4.716	0.016	0.965	0.719
C20	4.827	4.770	4.712	0.005	0.996	0.576
C24	4.849	4.766	4.684	0.018	0.963	0.828
C25	4.520	4.451	4.382	0.006	0.992	0.690

General equations of density as a function of sulfur content and matte grade were calculated from the values above for each of the three temperatures. The equations are:

$$D_{1100} = 6.756 - 0.0927\ S + 0.0105\ G \quad SD = 0.0523 \quad ..12$$

$$D_{1200} = 6.605 - 0.0884\ S + 0.0099\ G \quad SD = 0.0465 \quad ..13$$

$$D_{1300} = 6.465 - 0.0845\ S + 0.0093\ G \quad SD = 0.0454 \quad ..14$$

where:

D_{1100} = density in g/mL at 1100°C

D_{1200} = density in g/mL at 1200°C

D_{1300} = density in g/mL at 1300°C

S = mass % sulfur

G = matte grade (mass % copper and nickel)

and SD = standard deviation in g/mL from density values in Table 3.

The densities of the matte specimens at each of the three temperatures, along with iso-density lines determined using the above equations, are shown in Figures 22, 23 and 24. The numbers beside each composition point in the Figures are: (Density - 4.00) x 100. Also, an overall empirical equation of density in g/mL, as a function of sulfur content, matte grade, and temperature has been calculated from the raw data, and is shown below.

$$D = 6.532 - 0.0856\ S + 0.0097\ G + 0.00049\ (1200-t) \quad ..15$$

The standard deviation of Equation 15 is 0.0496 g/mL.

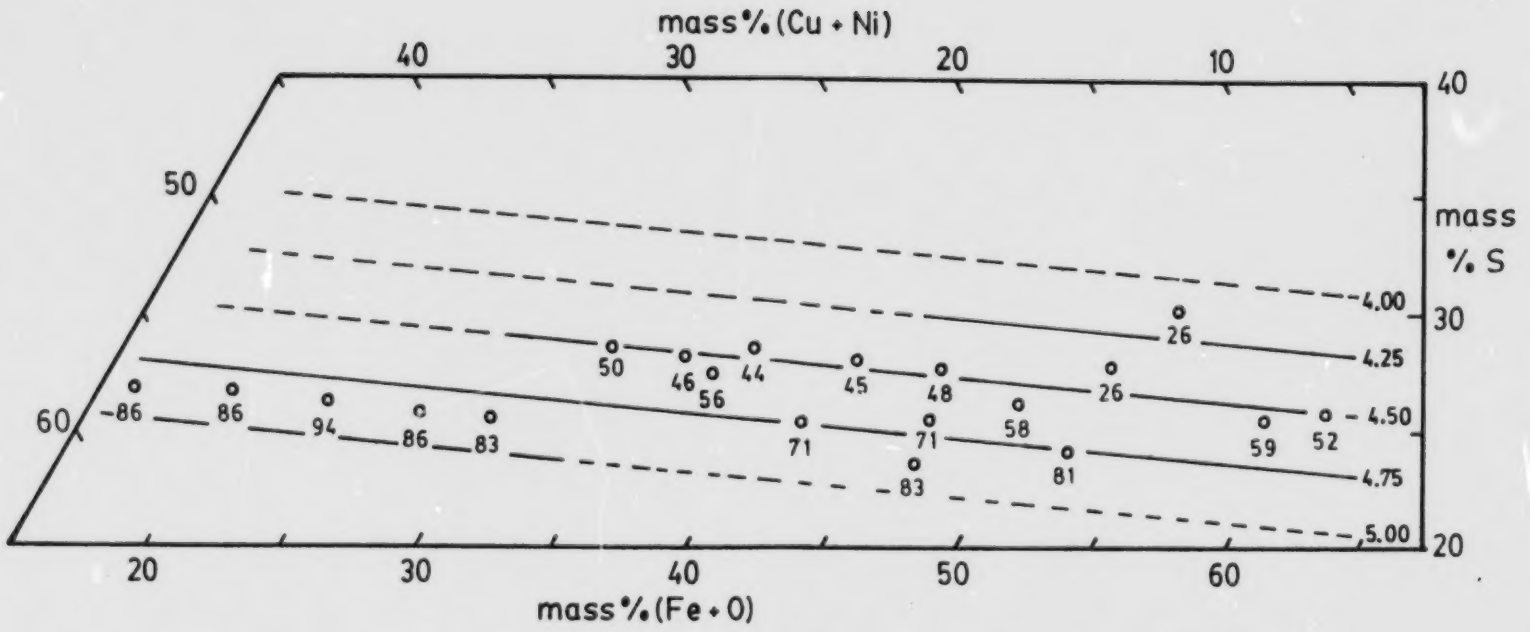

Figure 22. Densities of the matte specimens at 1100°C.

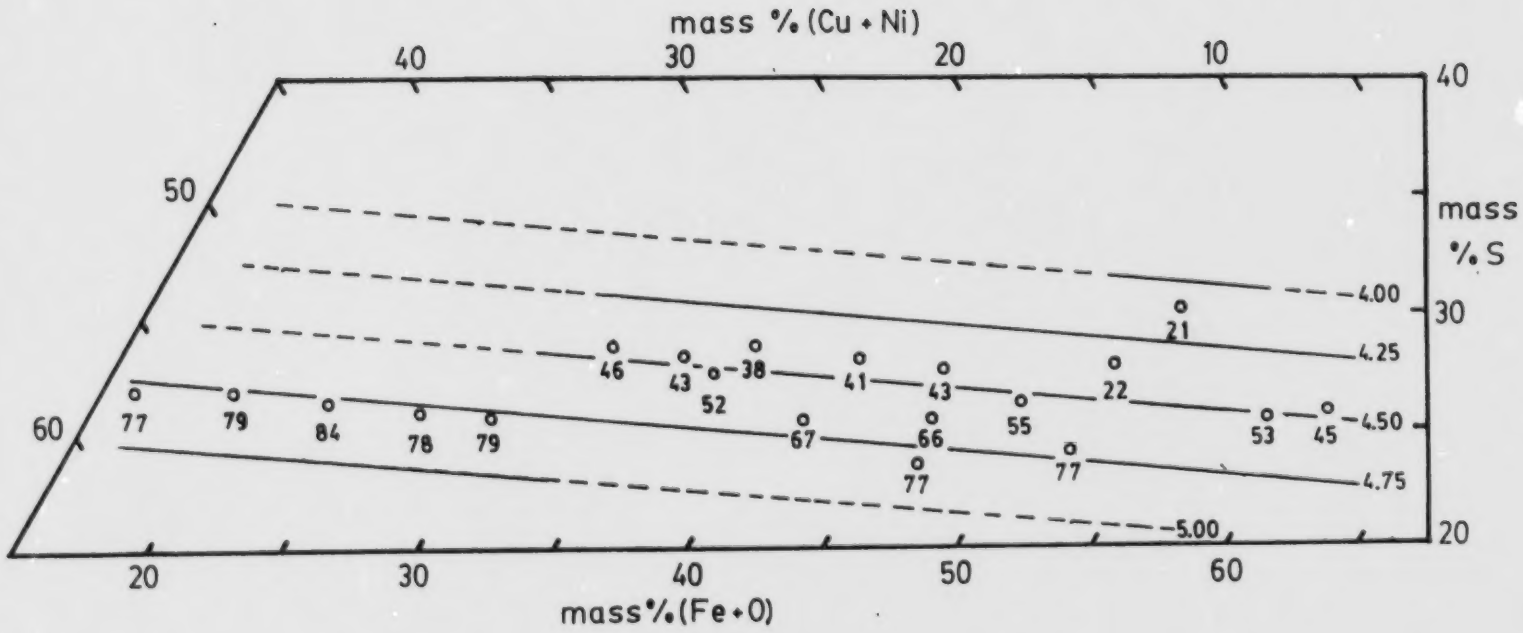

Figure 23. Densities of the matte specimens at 1200°C.

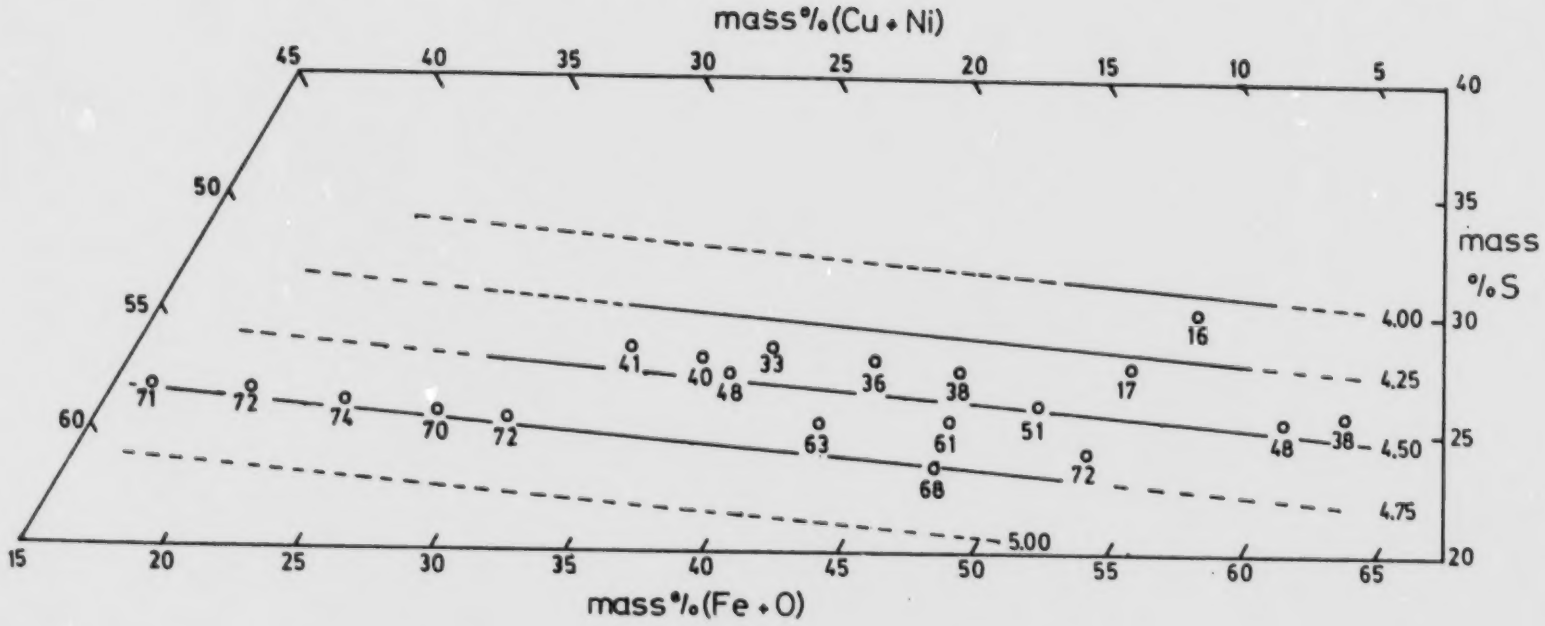

Figure 24. Densities of the matte specimens at 1300°C.

DISCUSSION

Archimedes' principle, when modified to a bottom weighing technique, is an effective method to determine accurately and precisely the densities of molten mattes. The accuracy of the method is enhanced because surface and interfacial effects, associated with the measurements, are eliminated. As outlined previously, these effects can substantially reduce the accuracy of the data obtained in using other methods. Other major factors that can affect the accuracy of the data are: the uncertainty of the matte volume displaced by the bobs, the uncertainty that the weight change indicated by the balance is a true indication of the displaced mass of the matte specimen, and the uncertainty of the matte composition whose density is being determined. Minor factors that affect the accuracy of the data to a degree less than the precision of the measurements, such as changes in atmospheric pressure and the earth's gravitational anomaly, will not be discussed.

i) Technique

a) Volume of Alumina Bobs

The volume of the alumina bobs was determined by immersing them into mercury, and measuring the displaced

weight on an electronic balance. Because of the high density of mercury, the relative error associated with the weight measurements is small. Also, the weight of displaced air is negligible in calculating the bob volume. Only the volume of the second upper bob must be determined precisely. The volume of the upper bob is deemed to include a small and precise length of the thin alumina rod, so that the bob also has a definite length. Using Equation 9, the volume of the upper bob was determined excluding any surface effect contributions, which arise from the interaction between the mercury surface and the alumina rod. Although the density of pure mercury is well established, it was not known how this density value changes with the absorption of gases into the mercury. The density of the mercury used was determined as accurately and precisely as possible, and with respect to the density of pure mercury, no difference in density was found to six significant digits. Therefore, the density value of pure mercury, as given in the literature, was applicable to the mercury that was used to determine the volume of the alumina bobs.

The bob volumes were also determined by immersion in water, not to increase the precision of the volume, but to determine the extent of porosity in the alumina, since the surface tension of matte is more similar to that of water than mercury. The alumina, from which the bobs were made, had a relative bulk density of 99.8+%, so it was not certain

if the matte would flow into the voids in the alumina bobs. Small bubbles on the surface of the bobs would indicate limited porosity. These bubbles were not visible, and, after the density measurements were made, the bobs showed no signs that matte had soaked into them, with the exception of a small amount of matte that soaked into the alumina cement. However, the matte volume that soaked in was small and it was believed that this volume did not cause a significant error in the displaced matte mass to the extent that the measurements would be systematically low, based on the precision of the density data reported.

The volume of the bobs was determined at room temperature to within the error given by the uncertainty of the balance readout for weights 'W_3' and 'W_4'. The volume of the bobs at high temperatures, however, was calculated using the value of the linear coefficient of thermal expansion of alumina ($LCTE_a$), as stated by the manufacturers. If this value was significanty in error, then there could be some systematic error involved with the volume of the bobs at high temperatures. Although the $LCTE_a$, as stated by the manufacturers, was not checked, this value would have to have been in error by about 1% in order to cause errors in excess of the stated precision, and it is unlikely that the degree of error in the $LCTE_a$ was greater than 1%.

b) Measurements

The typical balance readout as a function of the depth of bob immersion is shown in Figure 25. The force on the balance first decreases as the bob comes in contact with the matte surface. This is caused by the meniscus as it is drawn up to the bob. As the first bob is further immersed, the force due to the meniscus decreases as the contact angle of the bob to the surface increases. At the same time, the weight of the displaced matte increases, and the net force on the balance begins to increase. As the first bob becomes almost totally immersed, the net force on the balance is comprised of the weight of the displaced matte and the now maximum force exerted by the meniscus as the contact angle becomes almost 180^{o}. When the first bob becomes totally submersed, the net force on the balance decreases as the force of the surface effect sharply decreases. The force of the surface effect now is due only to the interaction of the thin alunima rod with the surface. This force does not change as the bob assembly is further lowered into the specimen. The net force on the balance increases slowly as the weight of the displaced mass increases. When the second bob comes in contact with the matte surface, the net force on the balance undergoes the same changes as with the first bob. When both bobs become totally submersed, the net force on the balance consists of a small surface effect due to the alumina rod, and the weight of displaced matte. When both

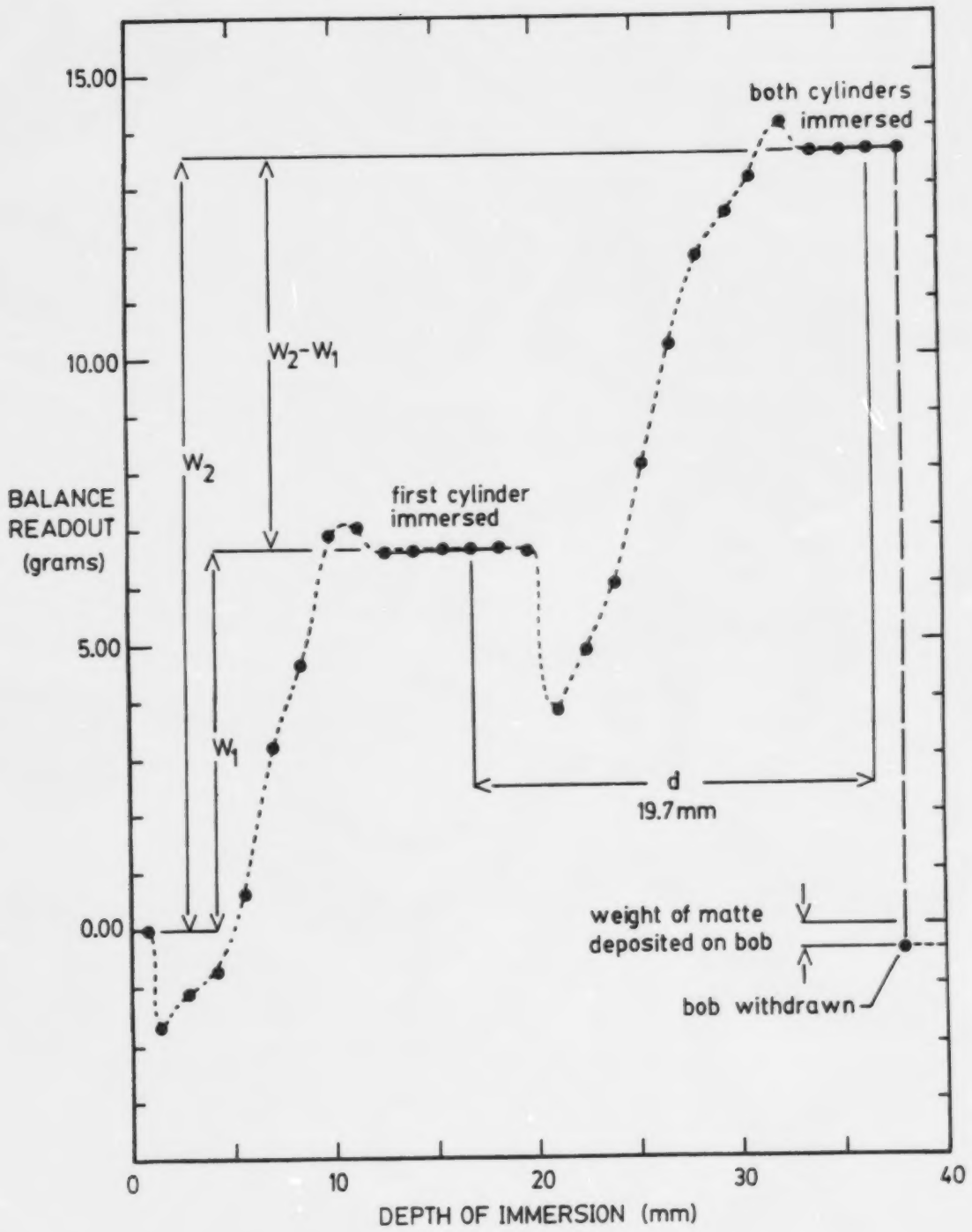

Figure 25. Balance readout versus bob immersion depth.

bobs are withdrawn from the matte, the net negative weight change is due to the matte that was deposited on the alumina bobs. This net weight change becomes zero if the bob assembly is immersed and withdrawn a second time.

The selected measurements were those that bracketed the main displacement body of the second bob, and at a specific length. The difference of these values does not contain a net surface effect contribution. In order to increase the accuracy of these values, a segment of the rod had to be included, even though this contribution is small in comparison to the large volume of the second bob. The measurements were made two or three times at each temperature, and, most often, these values were equal. The only instance where corrections were made to these values was when there was substantial sulfur evolution from the matte specimen. In that case, the rate of sulfur evolution was assumed to be constant with time at one temperature, and the appropriate amount of weight was added to the measurements, respecting the time at which the measurements were taken.

Measurements were discarded only when it was certain that they did not reflect the true displaced mass. An example of this would be when, at lower temperatures, the net weight loss would consistenty increase with each immersion and withdrawl sequence. It was assumed that this

indicated that some solidification of the matte was occurring and solid matte was becoming attached to the alumina bobs. Otherwise, all data points obtained were used.

c) Errors in the Measurements

Several factors could affect the accuracy of the measured weights indicated by the balance. One of these is lift on the crucible by the argon gas. The crucible containing the matte specimen sits on the supporting platform in the furnace hot zone. As argon gas flows by from beneath it, it gives the crucible a slight lift, which decreases the force on the balance. But because the argon flowrate is low at the time the measurements are being taken, the effect of this lift is not noticeable to the precision of the balance readout. The magnitude of this lift was checked by momentarily stopping the argon gas flowrate and observing any weight change on the balance readout. It was found that this source of error was negligible.

Another source of error arises from the fact that the density of argon at the matte temperature was not added to the calculated matte density in Equation 11. As is turns out, the density of argon is just less than the precision to which the density data are given. Therefore, adding the

value of the argon density to the calculated matte densities would not increase their accuracy.

A more significant source of error is that associated with the surface effect. The value of the surface effect could be calculated from Equation 7, since the volume of the first lower bob was known. But because of the relative magnitudes involved, the surface effect could be calculated only to within a 60% error. Nevertheless, the magnitude of the surface effect can lead to errors in the order of 0.03 g/mL in the calculated matte densities. This could have been a substantial error if it was not eliminated in this technique.

The last source of error in the recorded weight measurements is with the balance itself. Although the balance was calibrated by Fisher Scientific Co. Ltd., the calibration was checked prior to use. This was necessary because the weighing mechanism was not always perpendicular to the force of gravity. The manufacturer states that the deviation in the balance readout, with the balance inclined by 1:1000, is within 0.01 grams. When standard masses were placed into the crucible and weighed at various inclinations and altitudes, the balance reads between 99.96% and 100.04% of the actual mass. At a particular inclination, the deviation was always linear. The inclination of the balance, which is indicated by a bubble type circular level

mounted in the balance housing, was never allowed to exceed the degree which gave an error of 0.04%, which corresponds to a mass error of 0.003 grams in '$(W_2-W_1)/g$' in Equation 11. The balance has a reproducibility of 0.005 grams and a readability of 0.01 grams. This gives a total error in '$(W_2-W_1)/g$' of 0.023 grams. This value, combined with an error of 0.02 grams in '$(W_4-W_3)/g$', an error of 2 C^o in 't', and a 1% error in '$LCTE_a$', gives an estimated maximum absolute weight related error of 0.020 g/mL in 'D_{matte}' using Equation 11.

ii) Specimen Compositions

a) Initial Compositions

The B-series matte specimens were prepared by Falconbridge Ltd., using electric furnace matte as the starting material. As was previously mentioned, these specimens contained small amounts of cobalt. Because the density of cobalt sulfide is similar to that of iron sulfide, and because chemically, cobalt behaves similarly to iron in these mattes, it was decided to group the cobalt and iron assays together and to treat them as iron. This is justified because the cobalt assay is so small in comparison to the iron content.

The C-series specimens contained copper, nickel, iron,

sulfur, and oxygen. The effect on the matte density by other elements in these specimens, originating from impurities in the starting materials, is negligible because of their very low concentrations. The major impurity in the specimens is expected to be silica, arising from the imperfect separation of the sulfides from the pyrex tubes. Because the solubility of silica in mattes is small, and no silica type second phase was visible in the solidified mattes, the silica concentration in the matte specimens must have been very small. Therefore, the effect on the matte specimen density by the silica is expected to be negligible.

The C-series specimens were synthesized into matte just prior to determining their density in the furnace. The extent of sulfur evolution during fusion was minimized because of the way the sulfur was distributed among the three sulfides. Using the calculated metal- sulfur phase diagrams determined by Sharma and Chang[18,19,20], the sulfur potentials of the three sulfides mixtures were made as similar to one another as possible. This minimized any preferential sulfur evolution from the sulfide with a higher sulfur potential, which could result in an excessively sulfur deficient matte specimen.

b) Changes in Matte Composition

The uncertainty of the matte composition depends on

several factors. The most important of these is the change in specimen composition due to sulfur evolution from the matte in the furnace. With the bottom weighing technique, however, the extent of sulfur evolution was determined, since the weight of the matte specimen is continuously being monitored by the balance. In all cases, the change in the sulfur assay during the measurements was within the precision given in Tables 1 and 2.

The matte composition could also be affected by a chemical reaction between the matte and alumina crucible and bobs. The extent of intergranular corrosion of the alumina was minor, since the matte penetrated the alumina to a depth less than 0.1 mm. The matte did, however, partially soak through the Aremco Ceramabond alumina cement on the bob assembly. But because the quantity of matte absorbed was small, it was assumed that the composition of the matte specimen did not change nearly enough to affect the assays reported in Tables 1 and 2.

The last factor that could affect the composition of the specimen in the furnace is the oxidation or deoxidation of the matte by the argon cover gas. The oxygen in the argon was gettered by copper at 450°C to an oxygen partial pressure of about 10^{-10} atmospheres. With the specimen outside the furnace, the furnace atmosphere was purged with the deoxidized argon. When the specimen was raised into the

furnace hot zone, the oxygen potential of the surrounding gas was already low. Excess oxygen would oxidize the sulfur in the specimen primarily to SO_2, which would escape as gas and decrease the force on the balance. Oxygen could also dissolve into the matte and thereby increase the force on the balance, if the oxygen potential of the matte was very low. Because the oxygen level in the matte specimens was fixed either by magnetite (in C-series specimens) or by air (in B-series specimens) to values typically found in industrial mattes, it is highly unlikely that a significant amount of oxygen from the surrounding gas would be able to dissolve into these matte specimens. And because the sulfur partial pressure in these mattes is in the same order of magnitude as the oxygen partial pressure, sulfur oxidation would occur prior to specimen deoxidation. Therefore, when no weight change is being recorded by the balance, no oxidation or deoxidation of the specimen is ocurring to a significant degree.

c) Sampling Methods

It is believed that the greatest error in the matte specimen compositions stems from the sampling method. The first thirteen matte specimens (B-series) were sampled by grinding the entire specimen and removing a representative matte sample. The assays of these samples appear to be accurate. However, the remaining seven specimens (C-series)

were sampled by removing several central portions of the solidified matte, grinding them and obtaining representative samples. It was later determined that during solidificaion, oxygen, in the form of magnetite, preferentially collected on the matte specimen surface in a thin layer. Because this surface was excluded during sampling of these mattes, the oxygen assay determined was about 50% low, based on the amount of oxygen that was added to the specimens. This was especially true for the specimens with relatively high oxygen contents since the initial oxygen level of these synthesized mattes was known fairly accurately.

iii) Matte Density as a Function of Temperature and Composition

The densities of the matte specimens were calculated using Equation 11. From these values, the density of each specimen composition was determined at 1100°C, 1200°C, and 1300°C using linear regression. Because of the relatively few data points at each composition, the inherent scatter of the data, and the relatively narrow temperature range that was investigated, it was not possible to determine generally if the matte specimen density was other than a linear function of temperature. Because the correlation coefficient, R, is not far from 1, and the standard error of estimate in Table 3 (0.003 to 0.018 g/mL) is less than the estimated experimental error (0.020 g/mL), it appears that the assumption of linear temperature dependence, for each specimen composition is justified. The values of Alpha, the temperature coefficient of density in Table 3, vary considerably over the range of composition investigated.

Examination of the data, however does not seem to indicate any significant correlation of Alpha values with either (Cu + Ni) mass % or with S mass %, although because Alpha is small, the relative errors associated with it are large. Nevertheless, Alpha is assumed to be independent of composition.

Using the calculated values of the specimen densities at 1100°C, 1200°C, and 1300°C, Equations 12, 13, and 14 were determined. These general equations, plotted in Figures 22, 23, and 24, can be used to predict the densities of mattes at the above temperatures. The figures show a reasonable fit between the data and Equations 12 - 14, and this is confirmed by the relatively low values of the standard deviation in the equations.

Incorporating temperature as a linear relationship, the empirical Equation 15 is determined. To estimate the matte density at various compositions and temperatures, the empirical equations should be interpolated. Although interpolation of the empirical equation can give fairy accurate density values, extrapolation to values outside the composition and temperature ranges investigated can be misleading because of the uncertainty in the accuracy of Equation 15.

CONCLUSIONS

1. The bottom-weighing technique based on Archimedes' principle is a superior method to determine densities of molten mattes because surface and interfacial tension effects are eliminated.

2. At constant matte grade, sulfur in mattes decreases the density by 0.0856 g/mL per 1 mass % S, while at constant sulfur content, copper and nickel increase the density of the matte by 0.0097 g/mL per 1 mass % (Cu + Ni).

3. The temperature coefficient of density is similar over the range of compositions investigated and corresponds to a decrease of 0.00049 g/mL/C^{o} in the range 1100^{o}C - 1300^{o}C.

4. The empirical equation for density of mattes as a function of composition and temperature was determined by linear regression to be:

$$\text{Density} = 6.532 - 0.0856\ \%S + 0.0097\ \%(Cu + Ni) + 0.00049\ [1200 - t(C^{o})]$$

5. The analytical error of each data point was estimated at 0.02 g/mL absolute. The standard deviation of the empirical equation is 0.05 g/mL.

REFERENCES

1. "Densities of Molten Cu-Fe Sulfide Mattes." M. Bourgon, G. Derge, and G. M. Pound. Transactions of The Metallurgical Society of AIME. June 1958, pp. 338-40.

2. "Determining Melt Density by a Method which Forces the Melt to Rise in a Capillary Tube." M. N. Travnichek and F. M. Chernomurov. Tsvetnye Metally. / Non-Ferrous Metals. May 1973, pp. 22-3.

3. "Densities of Molten Nickel Mattes." J. J. Byerley and N. Takebe. Metallurgical Transactions. Vol. 2, April 1971, pp. 1107-1111.

4. "Densities of Molten Copper Mattes. I." K. Azuma and N. Takebe. Nippon Kogyo Kaishi. Vol. 88, 9 1972, pp. 557-62 (43-8). (Jap.).

5. "Measurements of Density and Surface Tension of Copper Mattes." S. Tokumoto, A. Kasama, and Y. Fujioka. Osaka Daigaku. Kogakubu. / Technology Reports of the Osaka University. Vol. 22, 1972, pp. 453-63.

6. An Attempt to Test the Theories of Capillary Action. F. Bashforth and S. C. Adams. Cambridge Univ. Press, 1883. (from 5.).

7. "Density of Molten Ag-S, Cu-S, Fe-S, and Ni-S Systems." M. Nagamori. Transactions of The Metallurgical Society of AIME. Vol. 245, Sept 1969, pp. 1897-1902.

8. "Density of Some Binary Liquid Metal Sulfides." L. N. Barmin, O. A. Esin, and I. E. Dobrovinskii. Thermodin. Svoistva Rasplavov. 1969, pp. 3-8. (Russ.).

9. "Application of Theory of Regular Solutions to Isotherms of Viscosity and Molar Volume in Binary Sulphide Melts." L. N. Barmin, O. A. Esin, and I. E. Dobrovinskii. Russian Journal of Physical Chemistry. Vol. 44, 10 1970, pp. 1450-3.

10. "Variation of the Volume and Viscosity of Sulphide Melts with Composition." I. E. Dobrovinskii, O. A. Esin, L. N. Barmin, and S. K. Chuchmarev. Russian Journal of Inorganic Chemistry. Vol. 14, 5 1969, pp. 727-30.

11. "Physicochemical Properties of Sulphide Melts." I. E. Dobrovinskii, O. A. Esin, L. N. Barmin, and S. K. Chuchmarev. Russian Journal of Physical Chemistry. Vol. 43, 12 1969, pp. 1769-1772.

12. "Physicochemical Properties of Cuprous Sulfide - Ferrous Sulfide System Melts. I." A. F. Kurochkin, M. T. Turisbekov, I. A. Onaev, and A. A. Kuzhamkulov. Vestn. Akad. Nauk Kaz. SSR. Vol. 28, 6 1972, pp. 38-46. (Russ.).

13. "Viscosity, Density and Surface Tension of Molten Iron and Copper Sulfide Mattes." Yu. V. Blagoveshchenskii, V. A. Bryukvin, V. N. Zheglov, V. G. Finikov, and O. I. Tsybin (Inst. Metall. im. Baikova, Moscow, USSR). Deposited Doc., 1976. VINITI 2929-76, 12 pp. (Russ.).

14. "Densities of the Molten FeS, FeS-Cu_2S, and Fe-S-O Systems -- Utilizing a Bottom-Balance Archimedean Technique." G. H. Kaiura and J. M. Toguri. Canadian Metallurgical Quarterly. Vol. 18, 1979, pp. 155-164.

15. Industrial data, courtesy Falconbridge Ltd., 1986.

16. "Some Viewpoints Concerning the Design of Electrical Resistance Furnaces." Lecture given by Chief Engineer Ture Thomander. Aktiebolaget Kanthal. Hallstahammar, Sweden. Catalogue BR:3 a 268, Appendix 5b.

17. Handbook of Chemistry and Physics, 64th ed. R. C. West, ed. CRC Press, Cleveland, 1983.

18. "A Thermodynamic Analysis of the Copper-Sulfur System." R. C. Sharma and Y. A. Chang. Metallurgical Transactions B. Vol. 11B, Dec 1980, pp. 575-83.

19. "Thermodynamics and Phase Relationships of Transition Metal-Sulfur Systems: Part III. Thermodynamic Properties of the Fe-S Liquid Phase and the Calculation of the Fe-S Phase Diagram." R. C. Sharma and Y. A. Chang. Metallurgical Transactions B. Vol. 10B, March 1979, pp. 103-8.

20. "Thermodynamics and Phase Relationships of Transition Metal-Sulfur Systems: Part IV. Thermodynamic Properties of the Ni-S Liquid Phase and the Calculation of the Ni-S Phase Diagram." R. C. Sharma and Y. A. Chang. Metallurgical Transactions B. Vol. 11B, March 1980, pp. 139-46.

APPENDICIES

APPENDIX A - Initial Compositions of B-series Specimens

SPECIMEN NUMBER	ASSAY (mass %) Cu	Ni	Co	Fe	S	O	TOTAL
B3	15.5	15.3	0.53	34.0	26.5	3.9	95.73
B6	8.2	8.4	0.11	49.0	28.0	3.1	96.81
B7	9.1	9.3	0.11	46.0	29.2	2.9	96.61
B12	11.4	13.0	----	45.0	25.3	2.5	97.2
B13	12.7	13.5	----	42.0	27.4	2.5	98.1
B14	14.0	14.9	----	39.0	28.0	2.3	98.2
B16	16.5	16.2	0.10	33.0	28.3	3.1	97.20
B17	16.1	15.3	0.10	38.0	25.0	2.6	97.10
B18	16.9	17.9	0.10	34.0	27.3	2.2	98.40
B19	18.3	18.7	0.08	30.0	28.0	1.9	96.98
B20	7.4	7.7	0.15	54.0	25.1	3.6	97.95
B21	11.9	11.4	0.12	47.0	24.3	2.9	97.62
B22	13.7	13.9	0.11	42.0	24.4	2.7	96.81

APPENDIX B - Target Compositions of C-series Specimens

SPECIMEN NUMBER	TARGET COMPOSITIONS (MASS %) Cu	Ni	Fe	S	O
C 16	21.35	21.35	30.4	25.0	1.9
C 17	22.80	22.80	27.2	25.5	1.7
C 18	24.25	24.25	24.0	26.0	1.5
C 19	25.70	25.70	20.8	26.5	1.3
C 20	27.15	27.15	17.6	27.0	1.1
C 24	14.10	14.10	46.4	22.5	2.9
C 25	6.30	6.30	59.2	24.5	3.7

On a 250 gram basis, the amount of starting materials, in grams, required to synthesize the metal sulfides is shown below. The sulfides are then combibed with magnetite to form the specimens.

SPEC.:	C16	C17	C18	C19	C20	C24	C25
Copper-sulfur mixture:							
Cu	53.375	57.000	60.625	64.250	67.875	35.250	15.750
S	13.469	14.384	15.299	17.892	21.663	8.895	3.974
Nickel-sulfur mixture:							
Ni	53.375	57.000	60.625	64.250	67.875	35.250	15.750
S	19.432	20.752	22.072	23.392	24.711	12.833	5.734
Iron-sulfur mixture:							
Fe	63.564	56.874	50.183	43.493	36.800	97.019	123.783
S	29.599	28.614	27.629	24.966	21.126	34.522	51.542
Magnetite:							
Fe_3O_4	17.185	15.376	13.567	11.758	9.949	26.230	33.466

APPENDIX C - Final Assays of Matte Specimens

SPECIMEN NUMBER	ASSAY (mass %) Cu	Ni	Co	Fe	S	O	TOTAL
B3	18.0	17.7	0.61	33.2	28.2	1.79	99.50
B6	8.4	8.5	0.10	50.4	30.6	3.57	101.57
B7	9.8	10.0	0.11	47.2	27.1	3.29	97.50
B12	11.9	12.3	0.12	46.3	25.9	2.29	98.81
B13	13.0	13.3	0.12	42.6	27.3	2.35	98.67
B14	14.5	14.9	0.10	39.9	28.0	2.27	99.67
B16	16.4	16.6	0.08	35.9	28.6	2.02	99.60
B17	16.1	16.7	0.10	39.4	25.3	1.87	99.47
B18	17.2	17.8	0.09	35.2	27.4	1.85	99.54
B19	18.8	19.2	0.07	31.2	28.4	1.54	99.21
B20	7.5	8.0	0.15	54.7	25.2	3.30	98.75
B21	11.4	12.1	0.12	49.4	24.0	2.12	99.14
B22	13.9	14.1	0.12	43.9	25.4	2.09	99.51

SPECIMEN NUMBER	ASSAY (mass %) Cu	Ni	Fe	S	O	TOTAL
C16	21.66	22.35	28.55	25.32	1.20	99.08
C17	23.38	23.22	25.80	25.77	1.38	99.55
C18	25.04	24.78	22.60	26.20	0.97	99.59
C19	26.19	26.72	19.30	26.50	0.59	99.30
C20	26.48	30.18	15.75	26.65	0.43	99.51
C24	14.61	14.45	44.25	23.18	1.71	98.20
C25	6.45	6.49	57.30	25.12	2.12	97.48

APPENDIX D - Raw Data

(W_4-W_3)/g grams	t C^o	W_1/g grams	W_2/g grams	(W_2-W_1)/g grams	D_{matte} g/mL
specimen no: B3					
22.29	1310	7.03	14.52	7.49	4.406
21.86	1305	7.01	14.35	7.34	4.403
21.86	1306	7.03	14.35	7.33	4.397
21.86	1231	7.10	14.46	7.36	4.423
21.86	1232	7.11	14.46	7.36	4.423
specimen no.: B6					
22.13	1310	6.69	13.66	6.97	4.130
22.13	1308	6.73	13.74	7.01	4.154
22.13	1243	6.78	13.84	7.06	4.190
22.13	1239	6.78	13.86	7.08	4.202
22.13	1178	6.81	13.91	7.10	4.221
22.13	1178	6.82	13.92	7.10	4.221
22.13	1120	6.84	13.96	7.14	4.251
22.13	1120	6.83	13.98	7.15	4.247
22.13	1077	6.86	14.01	7.15	4.261
22.13	1076	6.85	14.01	7.16	4.267
specimen no.: B7					
22.13	1307	6.70	13.73	7.03	4.165
22.13	1241	6.75	13.82	7.07	4.196
22.13	1241	6.75	13.83	7.08	4.202
22.13	1184	6.80	13.91	7.11	4.226
22.13	1184	6.80	13.91	7.11	4.226
22.13	1136	6.82	13.95	7.13	4.243
22.13	1135	6.82	13.95	7.13	4.243
22.13	1077	6.85	14.02	7.17	4.273
22.13	1077	6.84	14.00	7.16	4.267
specimen no.: B12					
21.61	1318	----	-----	7.43	4.507
21.61	1249	----	-----	7.46	4.533
21.61	1198	----	-----	7.46	4.539
21.61	1145	----	-----	7.49	4.563
21.61	1087	----	-----	7.52	4.588

(W_4-W_3)/g grams	t C^o	W_1/g grams	W_2/g grams	(W_2-W_1)/g grams	D_{matte} g/mL
specimen no.: B13					
21.92	1306	7.06	14.40	7.34	4.391
21.92	1310	7.16	14.45	7.29	4.361
21.92	1309	7.14	14.44	7.30	4.367
21.92	1248	7.17	14.53	7.36	4.409
21.92	1246	7.17	14.54	7.37	4.416
21.92	1192	7.19	14.61	7.42	4.452
21.92	1191	7.19	14.59	7.40	4.440
21.92	1137	7.22	14.63	7.41	4.452
21.92	1137	7.18	14.62	7.44	4.470
21.92	1083	7.23	14.68	7.45	4.482
21.92	1083	7.21	14.67	7.46	4.488
specimen no.: B14					
21.92	1301	7.10	14.40	7.30	4.368
21.92	1299	7.12	14.40	7.28	4.356
21.92	1216	7.19	14.52	7.33	4.395
21.92	1216	7.17	14.52	7.35	4.407
21.92	1152	7.21	14.59	7.38	4.432
21.92	1154	7.20	14.58	7.38	4.432
21.92	1079	7.26	14.66	7.40	4.452
21.92	1076	7.24	14.65	7.41	4.459
specimen no.: B16					
22.29	1318	6.85	14.19	7.34	4.317
22.29	1318	6.89	14.22	7.33	4.311
22.29	1318	6.89	14.26	7.37	4.334
22.29	1245	6.98	14.40	7.42	4.372
22.29	1243	6.98	14.36	7.38	4.348
22.29	1243	6.98	14.36	7.38	4.348
22.29	1187	7.02	14.48	7.46	4.402
22.29	1186	7.06	14.47	7.41	4.372
22.29	1185	7.02	14.46	7.44	4.390
22.29	1130	7.05	14.50	7.45	4.402
22.29	1129	7.03	14.53	7.50	4.432
22.29	1128	7.03	14.53	7.50	4.432
22.29	1073	7.09	14.61	7.52	4.450
22.29	1073	7.07	14.60	7.53	4.456
22.29	1072	7.07	14.64	7.57	4.480

(W_4-W_3)/g grams	t C^o	W_1/g grams	W_2/g grams	(W_2-W_1)/g grams	D_{matte} g/mL
specimen no.: B17					
21.98	1302	7.48	15.25	7.77	4.636
21.98	1302	7.52	15.29	7.77	4.636
21.98	1302	7.53	15.28	7.75	4.624
21.98	1231	7.58	15.37	7.79	4.656
21.98	1230	7.57	15.34	7.77	4.644
21.98	1176	7.58	15.41	7.83	4.687
21.98	1175	7.59	15.38	7.79	4.663
21.98	1122	7.61	15.45	7.84	4.699
21.98	1121	7.60	15.45	7.84	4.699
21.98	1060	7.62	15.49	7.87	4.724
21.98	1058	7.63	15.50	7.87	4.725
specimen no.: B18					
21.94	1319	7.26	14.75	7.49	4.475
21.94	1319	7.27	14.76	7.49	4.475
21.94	1250	7.34	14.86	7.52	4.501
21.94	1250	7.33	14.83	7.50	4.489
21.94	1192	7.38	14.92	7.54	4.519
21.94	1191	7.35	14.90	7.55	4.526
21.94	1135	7.40	14.96	7.56	4.538
21.94	1134	7.37	14.96	7.59	4.556
21.94	1086	7.39	14.99	7.60	4.568
21.94	1086	7.37	14.98	7.61	4.574
specimen no.: B19					
21.83	1309	7.09	14.40	7.31	4.391
21.83	1309	7.18	14.53	7.35	4.415
21.83	1310	7.20	14.55	7.35	4.415
21.83	1309	7.21	14.53	7.32	4.397
21.83	1245	7.26	14.64	7.38	4.440
21.83	1244	7.27	14.65	7.38	4.440
21.83	1244	7.26	14.65	7.39	4.446
21.83	1190	7.32	14.76	7.44	4.482
21.83	1190	7.33	14.74	7.42	4.470
21.83	1190	7.35	14.77	7.42	4.470
21.83	1135	7.38	14.83	7.45	4.494
21.83	1135	7.37	14.81	7.44	4.488
21.83	1135	7.38	14.81	7.43	4.482
21.83	1077	7.43	14.89	7.46	4.507
21.83	1075	7.41	14.86	7.45	4.501
21.83	1077	7.40	14.87	7.47	4.513

(W_4-W_3)/g grams	t C^o	W_1/g grams	W_2/g grams	(W_2-W_1)/g grams	D_{matte} g/mL
specimen no.:	B20				
21.77	1298	7.07	14.45	7.38	4.446
21.77	1296	7.21	14.69	7.48	4.507
21.77	1297	7.21	14.66	7.45	4.488
21.77	1235	7.27	14.75	7.48	4.514
21.77	1236	7.27	14.76	7.49	4.520
21.77	1235	7.27	14.75	7.48	4.514
21.77	1178	7.32	14.81	7.49	4.526
21.77	1178	7.30	14.80	7.50	4.532
21.77	1178	7.30	14.82	7.52	4.544
21.77	1119	7.30	14.89	7.59	4.593
specimen no.:	B21				
20.51	1299	7.27	14.64	7.37	4.713
20.51	1301	7.34	14.74	7.40	4.732
20.51	1300	7.34	14.73	7.39	4.725
20.51	1233	7.49	14.90	7.41	4.746
20.51	1232	7.40	14.83	7.43	4.759
20.51	1182	7.42	14.87	7.45	4.778
specimen no.:	B22				
21.89	1322	7.57	15.25	7.68	4.599
21.89	1321	7.54	15.23	7.69	4.605
21.89	1250	7.59	15.30	7.71	4.625
21.89	1249	7.59	15.32	7.73	4.637
21.89	1190	7.61	15.34	7.73	4.644
21.89	1192	7.61	15.37	7.76	4.662
21.89	1131	7.63	15.40	7.77	4.675
21.89	1131	7.63	15.42	7.79	4.687
21.89	1079	7.62	15.46	7.84	4.723
21.89	1079	7.62	15.47	7.85	4.729
specimen no.:	C16				
21.31	1301	7.37	15.03	7.66	4.714
21.31	1299	7.36	15.01	7.65	4.708
21.31	1299	7.37	15.04	7.67	4.721
21.31	1227	7.44	15.17	7.73	4.766
21.31	1227	7.44	15.17	7.73	4.766
21.31	1166	7.49	15.28	7.79	4.810
21.31	1165	7.51	15.31	7.80	4.817

(W_4-W_3)/g grams	t C^o	W_1/g grams	W_2/g grams	(W_2-W_1)/g grams	D_{matte} g/mL
specimen no.:	C17				
22.14	1290	7.57	15.48	7.91	4.687
22.14	1293	7.53	15.50	7.97	4.722
22.14	1290	7.56	15.53	7.97	4.722
22.14	1220	7.58	15.58	8.00	4.748
22.14	1218	7.60	15.62	8.02	4.761
22.14	1160	7.64	15.73	8.09	4.809
22.14	1160	7.63	15.73	8.10	4.815
22.14	1107	7.70	15.86	8.16	4.857
specimen no.:	C18				
22.73	1311	7.44	15.63	8.19	4.724
22.73	1313	7.45	15.65	8.20	4.730
22.73	1312	7.49	15.67	8.18	4.718
22.73	1251	7.54	15.79	8.25	4.766
22.73	1249	7.53	15.83	8.30	4.795
22.73	1197	7.60	15.93	8.33	4.819
22.73	1200	7.64	16.03	8.39	4.853
22.73	1198	7.65	16.06	8.41	4.865
22.73	1138	7.70	16.15	8.45	4.896
specimen no.:	C19				
22.20	1312	7.60	15.55	7.95	4.695
22.20	1311	7.58	15.57	7.99	4.719
22.20	1231	7.68	15.72	8.04	4.758
22.20	1231	7.69	15.76	8.07	4.776
22.20	1174	7.69	15.82	8.13	4.818
22.20	1172	7.72	15.81	8.09	4.795
specimen no.:	C20				
22.20	1302	7.66	15.63	7.97	4.708
22.20	1303	7.69	15.66	7.97	4.708
22.20	1235	7.77	15.80	8.03	4.752
22.20	1236	7.75	15.79	8.04	4.757
22.20	1175	7.83	15.89	8.06	4.777
22.20	1174	7.83	15.91	8.08	4.789
22.20	1121	7.87	15.98	8.11	4.813
22.20	1123	7.84	15.95	8.11	4.813
22.20	1073	7.89	16.05	8.16	4.848
22.20	1066	7.84	15.99	8.15	4.843

(W_4-W_3)/g grams	t C^o	W_1/g grams	W_2/g grams	(W_2-W_1)/g grams	D_{matte} g/mL
specimen no.: C24					
21.22	1324	7.58	15.09	7.51	4.639
21.22	1323	7.58	15.13	7.55	4.664
21.22	1269	7.62	15.24	7.62	4.713
21.22	1267	7.63	15.25	7.62	4.713
21.22	1219	7.68	15.38	7.70	4.769
21.22	1218	7.71	15.42	7.71	4.775
21.22	1168	7.74	15.46	7.72	4.787
21.22	1169	7.75	15.49	7.74	4.800
21.22	1116	7.78	15.53	7.75	4.812
specimen no.: C25					
21.67	1308	7.08	14.30	7.22	4.369
21.67	1306	7.13	14.38	7.25	4.387
21.67	1306	7.11	14.34	7.23	4.375
21.67	1235	7.16	14.46	7.30	4.425
21.67	1233	7.16	14.47	7.31	4.432
21.67	1169	7.24	14.60	7.36	4.469
21.67	1168	7.27	14.64	7.37	4.475